Fall 2021

# Development of a Rapid Compression and Expansion Machine To Characterize the Ignition Propensity of Multi-Component Liquid Fuels

Jonathan Joseph Morreale

# DEVELOPMENT OF A RAPID COMPRESSION AND EXPANSION MACHINE TO CHARACTERIZE THE IGNITION PROPENSITY OF MULTI-COMPONENT LIQUID FUELS

by

Jonathan Joseph Morreale

Bachelor of Science
University of South Carolina, 2018

---

Submitted in Partial Fulfillment of the Requirements

For the Degree of Master of Science in

Mechanical Engineering

College of Engineering and Computing

University of South Carolina

2021

Accepted by:

Sang Hee Won, Director of Thesis

Tanvir Farouk, Reader

Tracey L. Weldon, Interim Vice Provost and Dean of the Graduate School

## ACKNOWLEDGEMENTS

I would like to first thank the University of South Carolina for providing me with the necessary foundation from which I was able to build upon in this research. I would also like to thank Dr. Sang Hee Won for believing in me and allowing me to work in his lab. Without him believing in my ability, I would not be where I am. Finally, I would like to thank my family and friends for always being there to support me, picking me up when I'm down, and for pushing me to become a better person every day.

## ABSTRACT

Combustion has been the primary source for energy production, whether it be from coal, oil, or natural gas, for a very long time. With increasing population and therefore an increased demand for energy, efficiency is becoming a concern. In order to increase efficiency, engines have been downsized and compression ratios have been increased. In doing so, problems have arisen such as knock and low speed pre-ignition. To better understand these problems, an investigation into how fuels ignite at higher pressures is necessary. Real fuels are comprised of multiple components that exhibit significant variations in their own physical and chemical characteristics. Examining these characteristics of real fuels in real world applications has proved to be quite challenging due to the complexity associated with multi-component and multiphase combustion processes. The creation of a novel device to mimic the behavior of reciprocating engines is necessary to gather a fundamental understanding of these fuel properties and their impacts on multiphase combustion processes. The objective of this study is to develop a well-defined experimental platform that can provide high-quality measurements for both gas- and multi-phase ignition processes. Accordingly, a rapid compression expansion machine (RCEM) has been developed and its performance has been comprehensively evaluated. The RCEM is composed of a pneumatically driven actuator, cam, and combustion chamber. The actuator pneumatically pushes a cam that guides the piston to compress the combustion chamber. Pressure time-history profiles have been measured and used to evaluate the compression time for characterizing the polytropic compression

behaviors. Considering the relevance to the gasoline fuels, n-Heptane has been used as the primary fuel for this research, which represents the lighter components within an ethanol free fuel. This study summarizes technical challenges in developing a well-defined RCEM, along with experimentally observed ignition behaviors of both gas-phase and multi-phase mixtures.

# TABLE OF CONTENTS

# LIST OF FIGURES

# CHAPTER 1

## INTRODUCTION

In its many forms, combustion is the significant leader when it comes to energy production and transportation in the world and has been for the past 100 years. Combustion is the burning of hydrocarbons and other organic materials with the presence of oxygen to produce water and carbon dioxide. According to Our World in Data, in 2019, the primary combustion forms of gas, oil, coal, biomass and biofuels amounted to about 149,015 TWh of energy consumption. This was nearly 86 percent of the world's total energy production, which was 173,340 TWh, for the year with almost 92 percent of the combustion percentage coming from gas, oil and coal shown in figure 1.1 [1]. This number, although very large, makes sense because combustion has been around for a long time, which has allowed the knowledge of creating a combustion reaction easily accessed worldwide and has proven itself to be extremely reliable in producing energy at a low cost. Even though alternative and renewable energy sources are becoming more readily available as their respective technologies advance, the use of fossil fuels has also increased because the energy demand is growing faster than the rate in which those technologies advance. This trend can be seen in figure 1.2 [2]. Since the realization of using combustion for energy production and transportation, there has been a constant yearning for improving the processes to reduce emissions and increase efficiencies, mostly because it is the backbone of the world's economy.

Reliability, cost, and ease of access/production of creating energy from combustion are the primary reasons for its majority use around the world. Given these positive attributes, there are also some drawbacks that come along with combustion, with the two big ones being pollution and efficiency. Both pollution and efficiency have become the primary problems within the last few decades due to the ever-increasing world population. As the population has increased, the demand for energy has also increased, creating a positive feedback loop the continues to increase the population and energy demand. This is concerning because pollution of the world will lead to illness as air quality is decreased and the levels of toxic chemicals in soil and water sources rise. Efficiency of the combustion process is a problem because the increasing energy demand is depleting the resources required to fuel the reaction. If both of these problems can be improved upon, then combustion as the primary means of energy production can remain for decades to come.

Many people would argue that the switch to alternative energy sources needs to happen now so that the world isn't affected more than it already has been. However, what people don't realize is that making the switch is not that easy, especially in large countries like the United States. Infrastructure is the biggest obstacle that needs to be overcome in order to make a switch to a different energy source. Some smaller countries, by both landmass and population, have been able to make a switch to a majority of their energy production coming from renewable sources because the infrastructure requirements are not as great as the requirements for a large country. For example, Iceland produces 100% of its energy from renewable sources, with 73% coming from hydroelectric power and the remaining 27% coming from geothermal power. However, even though they have a

relatively small landmass and population, they are unique in that there is a lot of flowing water and volcanic activity on the island, making it possible to produce enough energy for its population. The building of infrastructure is the primary reason why the transition from combustion to alternative energy sources would be difficult because it would take a long time in larger countries with large populations. For this reason, combustion will still be the majority source of energy in these countries.

Another reason why combustion is the main source of energy production around the world is because of its simplicity ease of access, reliability, and cost. Countries around the world have utilized combustion as a means to boost their economy. This is in part due to the fact that combustion is a simple method of energy production, especially when compared to modern alternative energy sources such as solar and nuclear power. Since combustion has been around for so long, parts for creating simple engines can be had relatively easily and constructed with some simple teaching. Cost is another important factor for why developing countries have trouble rapidly transitioning to renewable energy sources. Reliability is perhaps the most important trait of combustion. Most alternative energy sources rely on weather patterns to generate their energy whereas the combustion reaction just needs to be initiated, whether it be in an engine or a turbine. Infrastructure, as mentioned before, is not only difficult for large scales, but it is also difficult in that it is expensive to upfit a country with renewable energy generators and storage systems.

With the number of countries that are still relying on the majority of their power coming from combustion, there are some concerns. The two main things to consider are the availability of resources and the pollution involved with the combustion process. Both of these concerns are important when looking at the future of the planet. Scientists today

are constantly checking the rate of fossil fuel consumption and comparing them to the estimated reserves remaining within the Earth's crust. According to the Organization of the Petroleum Exporting Countries, there was an estimated 1.5 trillion barrels of crude oil at the end of 2018 as seen in figure 1.3 [3]. That same year there was a consumption of 36.4 billion barrels. This translates to just over 41 years of crude oil remaining at the current rate of consumption. In order to prolong the life of combustion usage, efficiency increases need to be had.

The other major concern is pollution. It has been known since the end of the 19th century that greenhouse gasses exist. Molecules such as $CO_2$ and $H_2O$ absorb infrared radiation and contribute to the heating of the Earth's surface. Both CO2 and H2O are the products of combustion using hydrocarbons. Given the popularity of combustion around the world, the production of these greenhouse gasses will still be prevalent. This is why there is a push towards cleaner forms of energy such as solar and wind, but given the infrastructure requirements, it will be a long process.

The use of a Rapid Compression Controlled Expansion Machine (RCEM) will allow for controlled analysis of the combustion process and provide insight into how efficiency and emissions can be improved. Being able to analyze properties such as flame temperatures, emissions, preferential vaporization, and multiphase ignition under simulated real-world conditions at variable compression ratios will provide great insight into how fuels and powerplants can be improved.

Preferential vaporization and multiphase ignition are closely related to each other in real fuels that are comprised of many components. Lighter molecules tend to evaporate sooner than heavier molecules at a given temperature. If the temperature is not high enough

for the entire fuel to vaporize before ignition occurs, then the vaporized component will ignite before the liquid component. Multiphase ignitions caused by partial vaporization can lead to knock and low speed preignition especially as engines are downsized and compression ratios are increased. Understanding this phenomenon is a necessary step to ensuring that efficiencies in engines can be optimized and damage to engines is minimized.

Fossil fuels have paved the way for civilization by providing cheap, reliable energy that has industrialized and improved the quality of life for many nations. Despite the positive qualities, combustion's negative qualities have shown that it is not a permanent solution to the world's energy needs. Alternative energy sources are the future of powering the planet because many are emission free. The only reasons the switch has not yet been made is the cost and time that the switch over would require. The continued use of fossil fuels is the only viable solution for providing enough power to the world while the infrastructure for cleaner energy sources is developed. As more and more solar farms, wind generators, and other clean energy sources are built the use of fossil fuels can be tapered off until it is no longer needed. Until that day comes, combustion will continue to be researched and improved so that the quality of life for the world's population can be maintained.

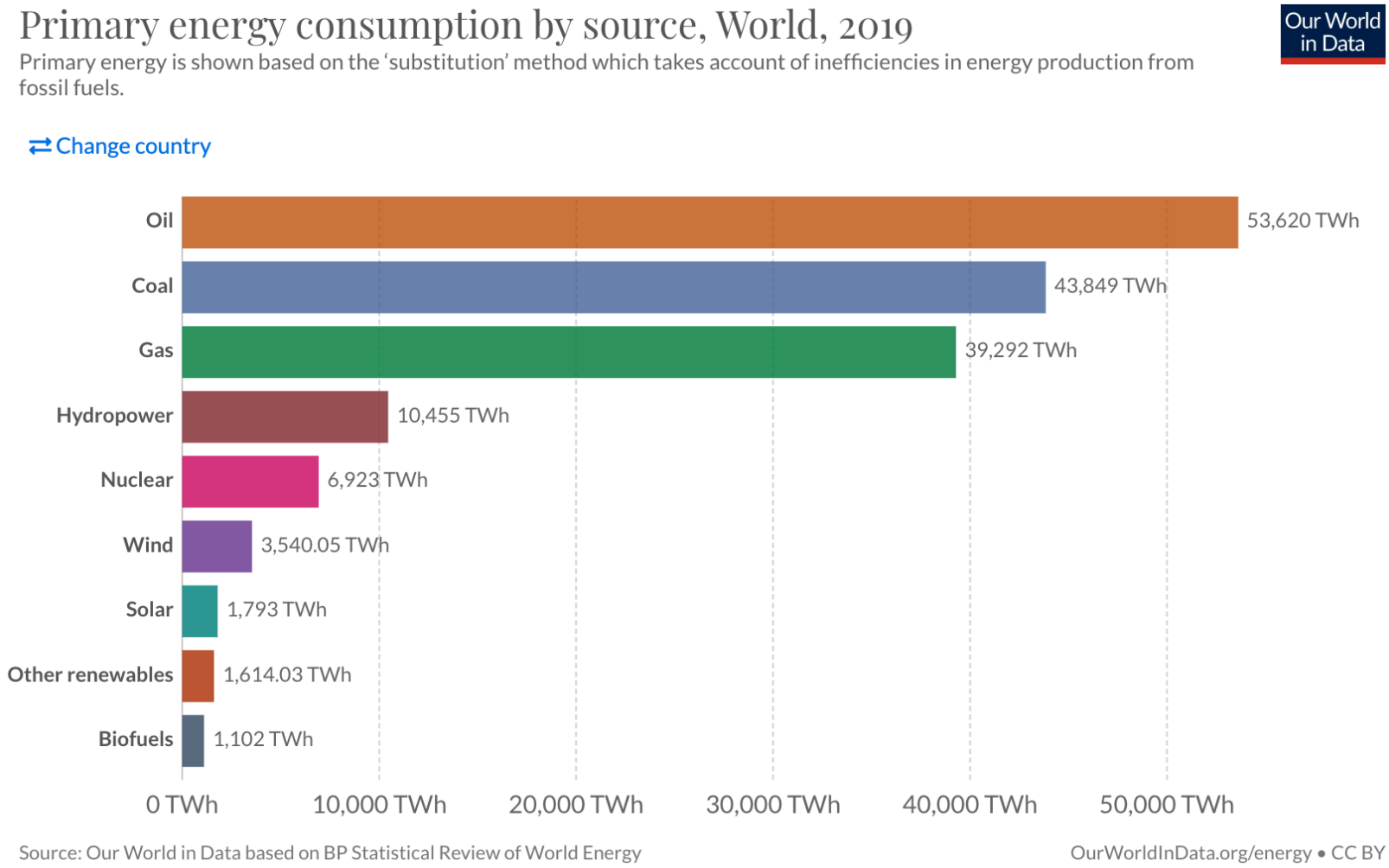


Figure 1.1: World energy consumption by source, 2019 [1]

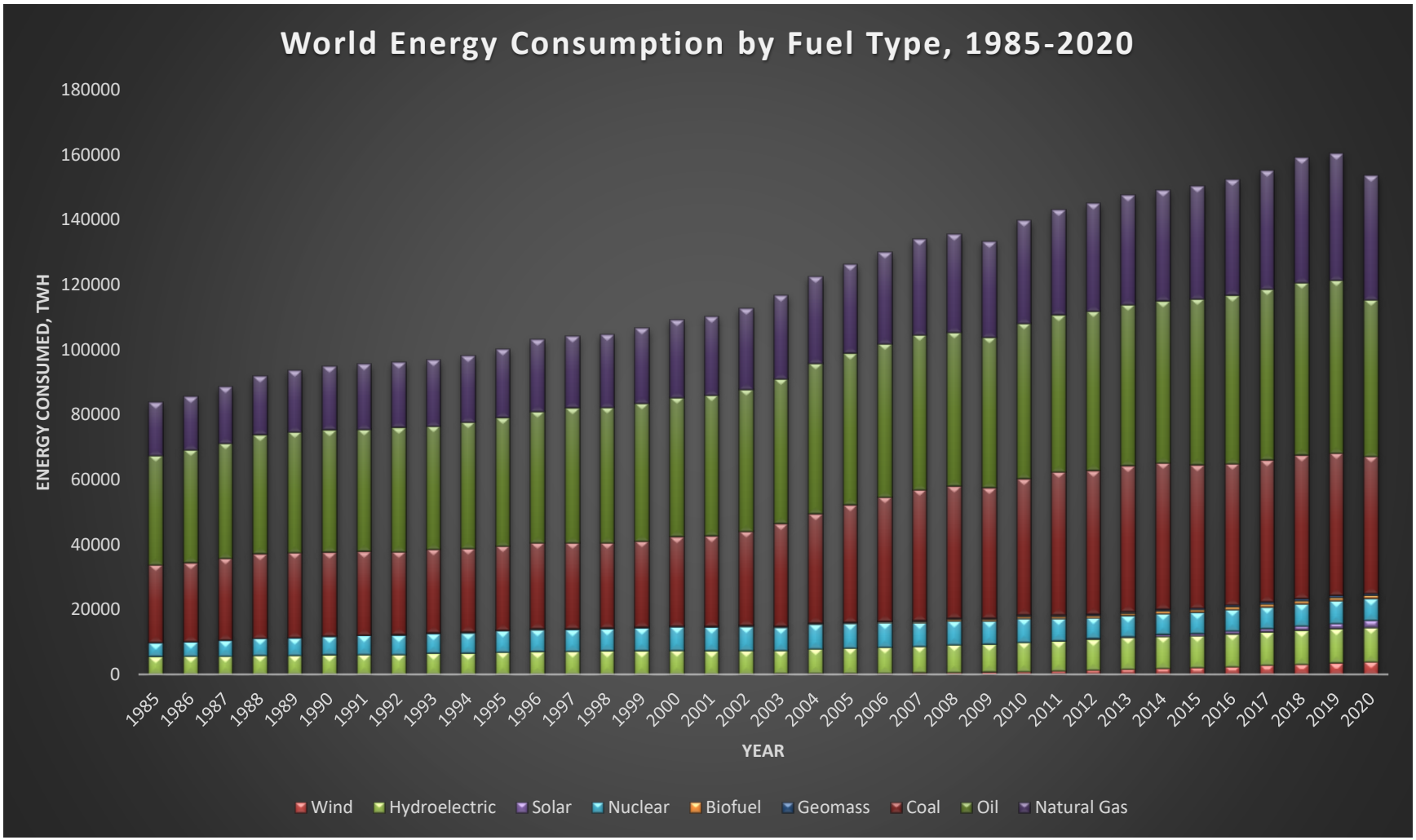


Figure 1.2: World energy consumption by source, 1985-2020 [2]

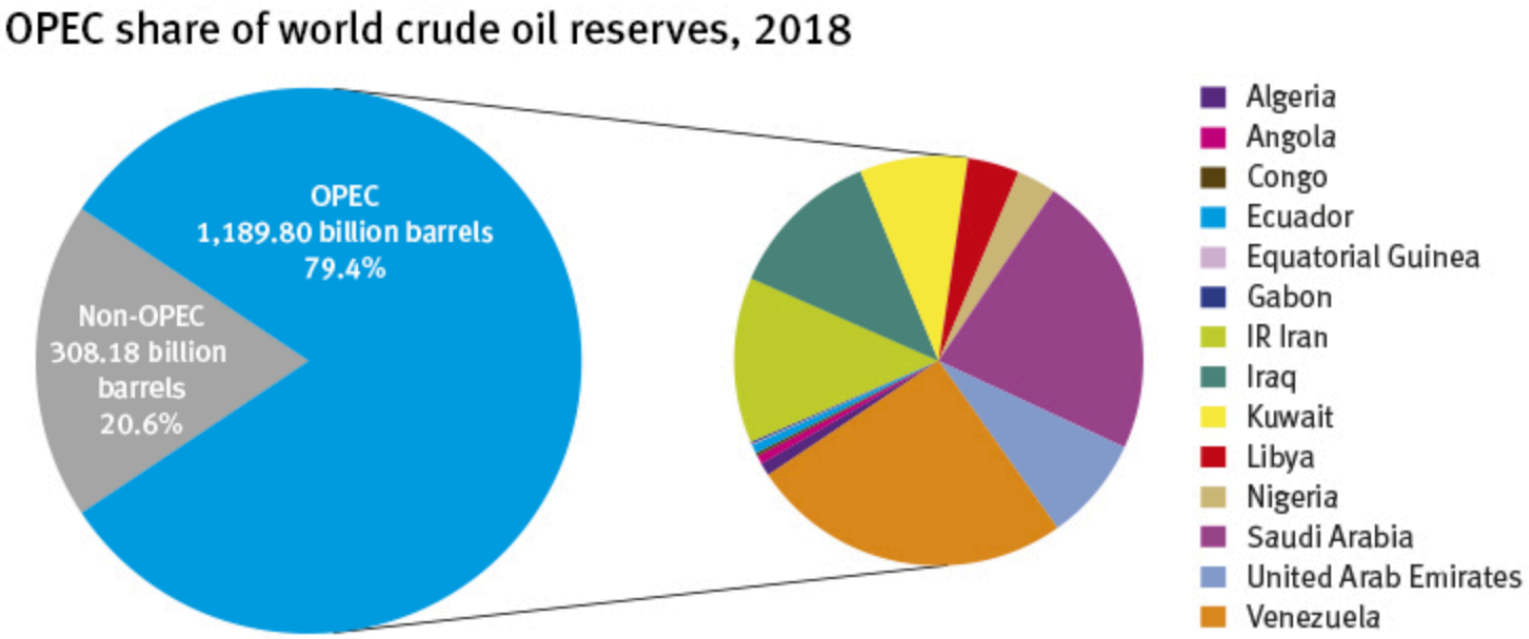


**OPEC proven crude oil reserves, at end 2018 (billion barrels, OPEC share)**

| | | | | | | | | | | | |
|---|---|---|---|---|---|---|---|---|---|---|---|
| Venezuela | 302.81 | 25.5% | Kuwait | 101.50 | 8.5% | Algeria | 12.20 | 1.0% | Gabon | 2.00 | 0.2% |
| Saudi Arabia | 267.03 | 22.4% | UAE | 97.80 | 8.2% | Ecuador | 8.27 | 0.7% | Equatorial Guinea | 1.10 | 0.1% |
| IR Iran | 155.60 | 13.1% | Libya | 48.36 | 4.1% | Angola | 8.16 | 0.7% | | | |
| Iraq | 145.02 | 12.2% | Nigeria | 36.97 | 3.1% | Congo | 2.98 | 0.3% | | | |

*Source: OPEC Annual Statistical Bulletin 2019.*

Figure 1.3: Estimated crude oil reserves for both OPEC and Non-OPEC countries as of 2018

# CHAPTER 2

# DESIGN

## RCM DESIGN

Although heavily influenced by other RCEM and RCM designs, the design for this machine proved to still be quite challenging. RCMs utilize an actuator, damper and combustion chamber that have traditionally been all oriented linearly. The actuation of the machine is usually performed with compressed air because of its availability and ease of controlling large amounts of force. Changing the amount of pressure introduced as well as the flow rate of the air being introduced can be used to explore the differences between varying compression times. The damper is used to slow down and eventually stop the piston, often through the use of controlled venting of hydraulic oil. Once the piston has stopped at the end of the compression stroke, the pneumatic actuator will hold the position of the piston throughout the remainder of the combustion process. A variety of sensors are utilized at the combustion chamber including pressure transducers, thermocouples, intake, exhaust, and windows to analyze different combustion properties. An example of an RCM can be seen in figure 2.1.

This design has been tried and tested and has produced many experimental results. However, RCM's have a constraint that limits their ability to reproduce the most accurate real-world conditions. The use of linear compression as well as the lack of an expansion component within the machine, hinders the ability of the machine to perform a full combustion cycle to occur that would be seen in internal combustion engines that utilize

cycles like the Otto cycle and diesel cycle. Both of these two issues were addressed by a different RCM design that changed the orientation of the actuator and combustion chamber from linear to a right angle with the utilization of a linear cam. The cam changes the compression rate from linear to more complex motions such as simple harmonic and double harmonic curves. The cam can also be used to include a period of expansion within the RCM process, creating something called a RCEM. Without the expansion component, the pressure is held much higher post-combustion and can lead to different intermediate reactions and final products. Adding the expansion process produces more realistic results.

**RCEM DESIGN**

The RCEM fixes this by introducing a controlled expansion portion within the process. Translation of linear movement by 90 degrees still occurs, similarly to the RCM's and RCEM's mentioned previously but the addition of the controlled expansion allows for a controlled temperature drop. The RCEM also utilizes an actuator, damper, and combustion chamber in a 90-degree orientation, but it differs in that the motion of the combustion piston is slowed simultaneously with the expansion portion of the process. This inclusion of a cam with expansion not only allows for a more complex compression, but also allows for the simulation of a piston expanding during the power stroke of a reciprocating engine. The piston's acceleration profile, when using a cam, can be more accurately represented than if the piston was directly attached to the actuator. This is because the crankshaft within an engine translates circular motion into linear motion. When this happens, starting from BDC, the piston's acceleration is lesser in the first 90 degrees of rotation than it is in the following 90 degrees of rotation. Once at TDC, the piston's acceleration becomes negative, and the acceleration profiles are flipped. The first 90

degrees, from TDC, will have a greater acceleration than the following 90 degrees of rotation [5]. The RCEM will allow for more accurate test results to be produced and hopefully some breakthroughs that can help increase efficiencies and reduced emissions. An image of the fully assembled RCEM can be seen in figure 2.2.

**TABLE**

The tables, that the RCEM and all of its components are attached to, are produced by McMaster-Carr, pictured in figure 2.3. The specific tables that the RCEM sits on top of were selected because of their tight flatness tolerances, heavy weight, rigidity, and ability to either be fixed to the ground with anchors or have feet attached such as castors for transportation or leveling/anti vibration mounts for uneven ground or extreme vibrations. The flatness tolerances of these tables are kept to a maximum of 0.002 inches per foot, meaning that the height across one foot of the tables surface will not change by more than 2 thousandths of an inch. The weight of each of the two tables is estimated to be just under 500 pounds without any components mounted to them. These estimates were calculated from the dimensions of the top plate which were 36 inches x 48 inches x ¾ inches resulting in a weight of roughly 367 pounds as well as each of the legs and supports which are constructed of 3-gauge steel and weigh roughly 127 pounds together. Due to the integration of a cam in the design of the RCEM, two tables were utilized to allow all of the components to be mounted to the tables. The actuator is mounted to one of the tables and the cam and combustion chamber are mounted to the other table. The heavy weight of these tables is important because of the large amount of force that is being applied from one table to the other with the actuator. In the first design iteration, the two tables were mounted together with 4 5/8”-11 threaded rods to ensure that the tables cannot separate during machine

operation. The rods did prevent the tables from separating, but they did not prevent them from rotating and skewing. This is important to correct because the alignment between the two tables is crucial to maintain repeatable data between experiments. To fix the movement issues, two parallel double aluminum extrusions were mounted between the tables and affixed on either end via 4 5/16”-18 bolts. This allows for not only better rigidity, but also a better guide rail mounting solution which will be discussed further in the cam profile section of this chapter.

A shelf underneath the table was constructed to house the DAQ cards, power supply, hoses, and other necessary equipment. This not only allows the electronic components to be stored out of the way, but also increased the weight of the tables which is useful in that it can reduce the vibrations generated from the operation of the RCEM. In its current state, the table is capable of performing in the way that it was intended to, and the addition of new components will only make the RCEM perform better.

**CAM PROFILE**

A few different cam designs were used throughout the testing of the RCEM. The first cam profile designed for use in this work consists of a compression and expansion period, which is illustrated in Figure 2.4. The compression period is a 9-inch simple harmonic rise over a period of 12 inches, which is coupled to a linear expansion period that drops 1 inch over a period of 12 inches. This cam profile allows for a compression ratio of up to 20:1 but can be reduced by changing the position of the cylinder which results in an increase of the initial volume of the cylinder as well as a larger volume when the piston is at top dead center. This cam was manufactured by Metro Machine Works, Inc. and is made of 4140 steel which was cut using a waterjet to save money. Its overall dimensions are

approximately 34 inches x 10.5 inches x 0.75 inches. It weighs just over 32 pounds, which is largely due to the inclusion of large weight cutouts within the main body of the cam.

The second cam design was created in an attempt to increase the compression ratio and reduce the compression time. The compression period for this cam is a 11-inch double harmonic rise over a period of 9.5 inches and the expansion period was removed to allow for the temperature to remain higher for longer. Just like the first cam, this one was manufactured by Metro Machine Works, Inc., but this time the material chosen was carbon steel a36 and machining was done on both a waterjet and CNC mill. The waterjet was used to get the general shape and the CNC mill was used to make the holes and to create a smooth surface for which the roller will ride along. This cam is pictured in figure 2.5.

The third and final cam used in this research is an improved version of the first cam design. Just like the first cam, it features a 9-inch simple harmonic rise over a period of 12 inches and was made by Metro Machine Works, Inc., however this version lacks an expansion period just like the second cam. The machining for this version was done similarly to the second cam, where the waterjet was used to produce the general shape and the CNC mill was used to get a smooth finish along the roller surface and to produce the holes from a blank of a36 carbon steel. The biggest improvement with this design was the inclusion of a roller holder which solved a big issue that the first 2 cams had. This issue will be discussed further in the assembly and performance verification chapter. This cam is shown in figure 2.6.

The cam assembly consists of the cam along with four linear slide bearings which ride along two guide rails that are mounted to the table via two double slot 1.5-inch aluminum extrusion with dedicated adapter inserts. Both rails are mounted parallel to each

other 7 inches apart which coincides with the mounting hole locations on the cams. The parallel support fastens directly into the tabletop, while the rear support structure, which is made of two 6-inch by 8-inch steel corner brackets with the bottom surface mounted to the table and the vertical surface mounted to the guide rail. The design of the cam assembly is ideal to prevent deflection throughout a large range of operating conditions, as well as to ensure a high degree of reliability. A high-load sealed ball bearing is used as a follower for the connecting rod to ride along the cam. The bearing is held in place by a 0.5-inch diameter by 6-inch-long stainless-steel rod that runs through the connecting rod and is held in place by a not on either side. The connecting rod is 1.375 inches in diameter and is made out of 4340 steel. This rod runs through a high-load linear ball bearing that is mounted to the table just before the beginning of the cylinder (see figure 2.7). The creviced-piston assembly described later in this section threads directly onto the opposite end of this rod.

**PNEUMATIC ACTUATOR**

Driving the cam assembly is a large-bore, custom pneumatic actuator built by Peninsular Cylinders and Dover Hydraulics (figure 2.8). This actuator features an 8-inch diameter piston which can produce just over 12,500 pounds of force at a maximum driving pressure of 250 psi. The driving side of the pneumatic actuator is fitted with a 3-inch NPT port, which connects to an 80-gallon receiver tank by way of a 1.5-inch hose that splits to divert air to the front and rear of the actuator. The tank was sized in order to maintain more than 87 percent of the driving pressure throughout the 30-inch compression stroke. Driving pressure is set by regulating the building air supply to a value within the operating ranges of 10 psi and 140 psi. This range is set by the solenoids, which require a difference in pressure on either side to operate, and the material limitations of the cam follower. In order

to prevent pressure from building up in the front side of the actuator, a ¾ inch NPT port was added as a vent. This port is fitted with an individual ball valve, which is used to pressurize the front side of the piston in order to retract the RCEM. The pneumatic actuator drives a rod that is 2 inches in diameter and has 1 ¼ - 12 by 2-inch female threads machined into the end.

**PISTON**

The combustion chamber is 2 inches in diameter and has a standard clearance height of 0.7 inches. The volume trajectory of the combustion chamber is governed by the cam profiles described in the previous section. The cylinder and head are made of 304 stainless steel, while the creviced-piston assembly is made out of 6061 aluminum and Buna-N u-cup seals. The piston used is a numerically optimized design developed by Mittal and Sung [9]. The creviced piston is used to limit adverse fluid dynamics caused by using a flat piston, which causes cool boundary layer gases to shear off the cylinder wall during compression. The boundary layer gasses shearing off the cylinder wall creates a vortex which flows over the top of the piston and results in a nonhomogeneous compressed temperature field. An exploded view of the piston assembly can be seen in Figure 2.9, which shows the three aluminum pieces as well as the two u-cup seals. The u-cups are important in this assembly because they are what allow the air within the cylinder to compress. The u-cup closest to the top of the piston is placed facing away from the combustion chamber, while the other u-cup is placed facing the combustion chamber. This is important because bottom u-cup allows for compression, while the top u-cup allows for a vacuum. This assembly then threads directly onto the connecting rod. Having the piston

as a separate part from the connecting rod allows for the piston to be swapped out should it incur damage or if alternative piston designs need to be tested.

**CYLINDER**

A schematic of the cylinder head is shown in figure 2.10. The cylinder was designed with versatility in mind. Six instrumentation ports have been designed using 3/4"-10 bolts with 1/8” NPT holes added to the head to allow for the pressure transducer, thermocouple, droplet tether and fuel injection port to be attached as well as allowing for the attachment of two additional instruments if the need should arise. The ports that are not currently in use are occupied by standard 3/4"-10 stainless steel bolts so that there is no dead volume. At the head of the cylinder, a recess was designed to allow for the use of an optical window. During initial testing, a metal plate, of the same dimensions as the optical window, was used to ensure that the window would not be damaged.

In order to increase the compression ratio of the RCEM, a number of inserts were designed to reduce the volume at TDC. A total of 3 inserts were made, each with its own dimensions, so that the best layout could be determined. The first of which was a Teflon ring with an outer diameter of 1.98”, inner diameter of 1” and thickness of 0.3”. This was then wrapped in Teflon tape to increase the diameter slightly so that the insert fit snugly at the head of the cylinder, just in front of the thermocouple and droplet tether. The second insert was also made of Teflon and had the same diameter dimensions as the first, but this time the thickness was increased to 0.8”. 6 1/8” Holes were placed evenly around the circumference of the insert to allow for pass-through of the thermocouple and droplet tether. The holes were made 0.5” off of one side of the insert so that the insert would be flush with the optical window. This insert also needed to be wrapped in Teflon tape to

secure it in place. The third insert, pictured in figure 2.11, was made of stainless steel and also had the same diameter dimensions as the first 2 inserts, but the thickness was reduced to 0.7". The same 1/8" holes were added to 4 of the hole positions around the circumference of the insert. The other 2 holes that were added were 5/32" to allow for a 1/8" diameter thermocouple to be inserted through without resistance. Again, the hole positions were placed 0.5" from one of the faces of the insert so that it would be flush with the optical glass. Additionally, 3 evenly spaced set screw holes were added to the insert around the circumference so that it could be held in place without the use of Teflon tape. To further increase the compression ratio with the use of these inserts, 1" quartz discs of varying thickness were added into the inner diameter of the inserts. The largest of which was a 3/8" thick disc so that there was still clearance for the thermocouple and droplet tether.

**SENSORS**

To record pressure data, the cylinder head was initially fitted with a Kistler 601CAA piezoelectric pressure transducer. This pressure transducer was chosen because of the high sample rate and its ability to operate in high pressures. However, the transducer was eventually swapped out for an Ashcroft G2 pressure sensor after the piezoelectric crystals within the sensor were damaged. This was going to be a temporary solution while the Kistler sensor was going to be either repaired or replaced, but after discussing the issues with Kistler, the damage was discovered to have come from the high temperature of combustion. Even if the temperature is high for a small amount of time, the crystals can become damaged which can result in the pressure reading to creep when no load is being applied. Given the low price of the Ashcroft pressure transducer, it made more sense for it to become the new primary sensor, as if it got damaged, it was not as big of a financial hit.

The Ashcroft pressure transducer has a sample rate that is a factor of ten less than the Kistler sensor, but this has not been a problem because the sample rate is still fast enough to record the pressure throughout the compression and combustion [9, 10].

A type-K thermocouple is used to record temperature data within the combustion chamber prior to, during and after a test. This is most important for knowing the temperature before a test is performed because the cylinder is heated with heating tape. The temperature can be recorded during the test, but the temperature data is not very accurate due to the diameter of the thermocouple not being small enough. The smaller the diameter is of a thermocouple, the quicker the temperature changes within the thermocouple bead and therefore the temperature can be read at a quicker rate.

### CONTROL SYSTEM AND DATA COLLECTION

The control system and the data collection system are one in the same. This is due to the use of LabView which allows for the integration of sensors into a user interface so that the RCEM can be controlled and the data from experiments can be recorded. The user interface (figure 2.12) of the LabView program was designed so that all pertinent data from the atmospheric conditions and experiment could be seen in real time. Once the run button is pressed, the live data starts to be shown and the entire system is initialized. Pressure data is shown for the cylinder as well as both the front and rear of the actuator. The cylinder pressure is important because it allows for leak testing and to see if the cylinder is at atmospheric conditions before an experiment ensues. The actuator pressure being shown allows for the user to know if either side of the actuator is pressurized, which is important for safety when disconnecting the hoses.

After the run button is pressed, 3 main buttons become activated, being manual control, fire and initialize. Manual control allows the user to activate each of the 4 solenoids that control the air flow direction and venting of the actuator. This button also locks the fire and initialize buttons when pressed to act as an additional level of safety. The fire button is used to begin the experiment by controlling the solenoids in a way that allows air to enter the rear of the actuator and allow air to exit the front of the actuator. When this happens, the actuator moves forward which causes the piston to compress the air in the cylinder. The initialize button resets the RCEM back to its initial position so that another experiment can be run. This is done by activating the solenoids opposite of the ones that were activated during the fire process. Just like with the manual control button, once the fire and initialize buttons are pressed, the other buttons are locked to prevent interruptions in the experiment and reset.

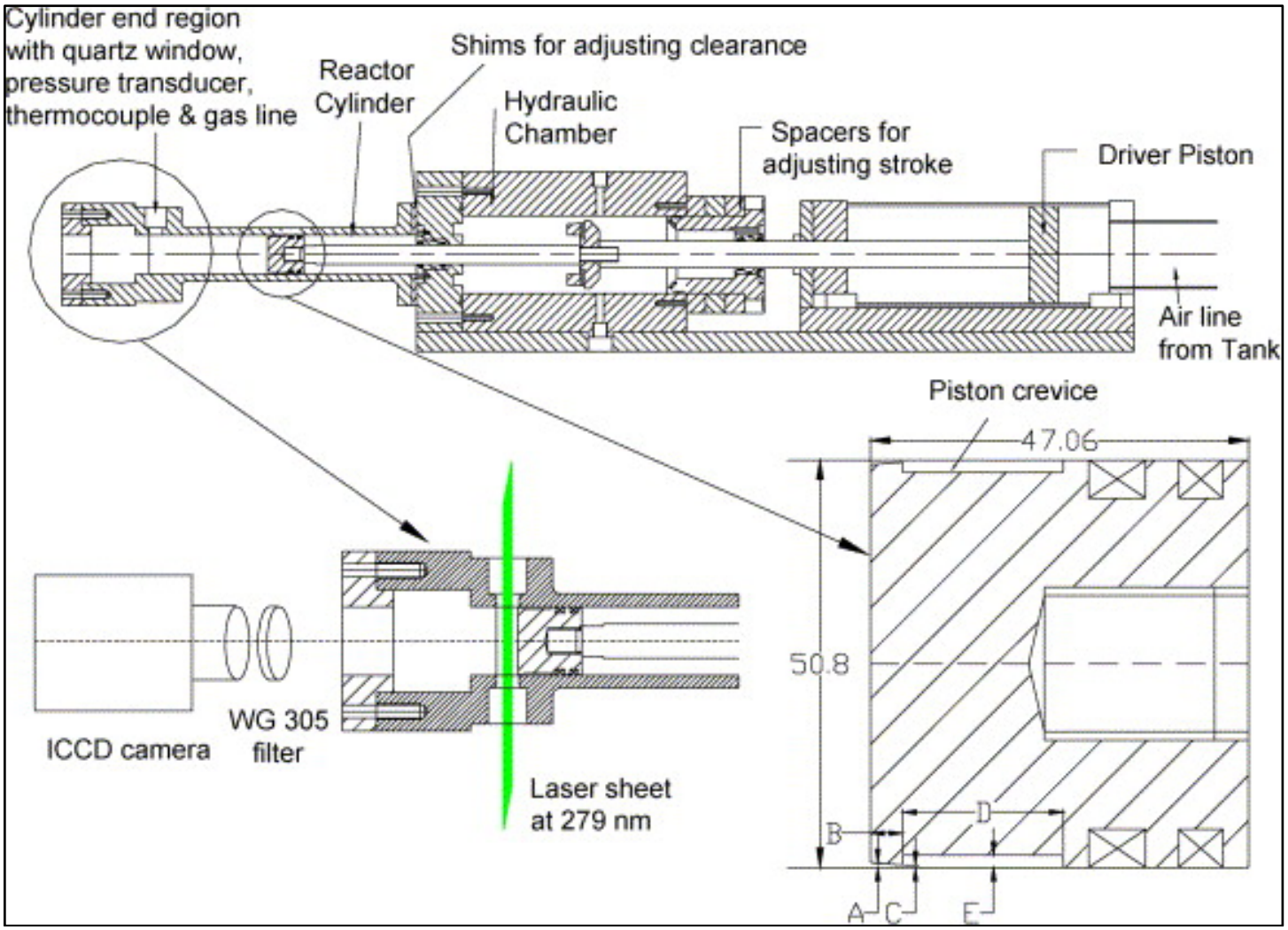


Figure 2.1: Schematic diagram of rapid compression machine (RCM) [9]

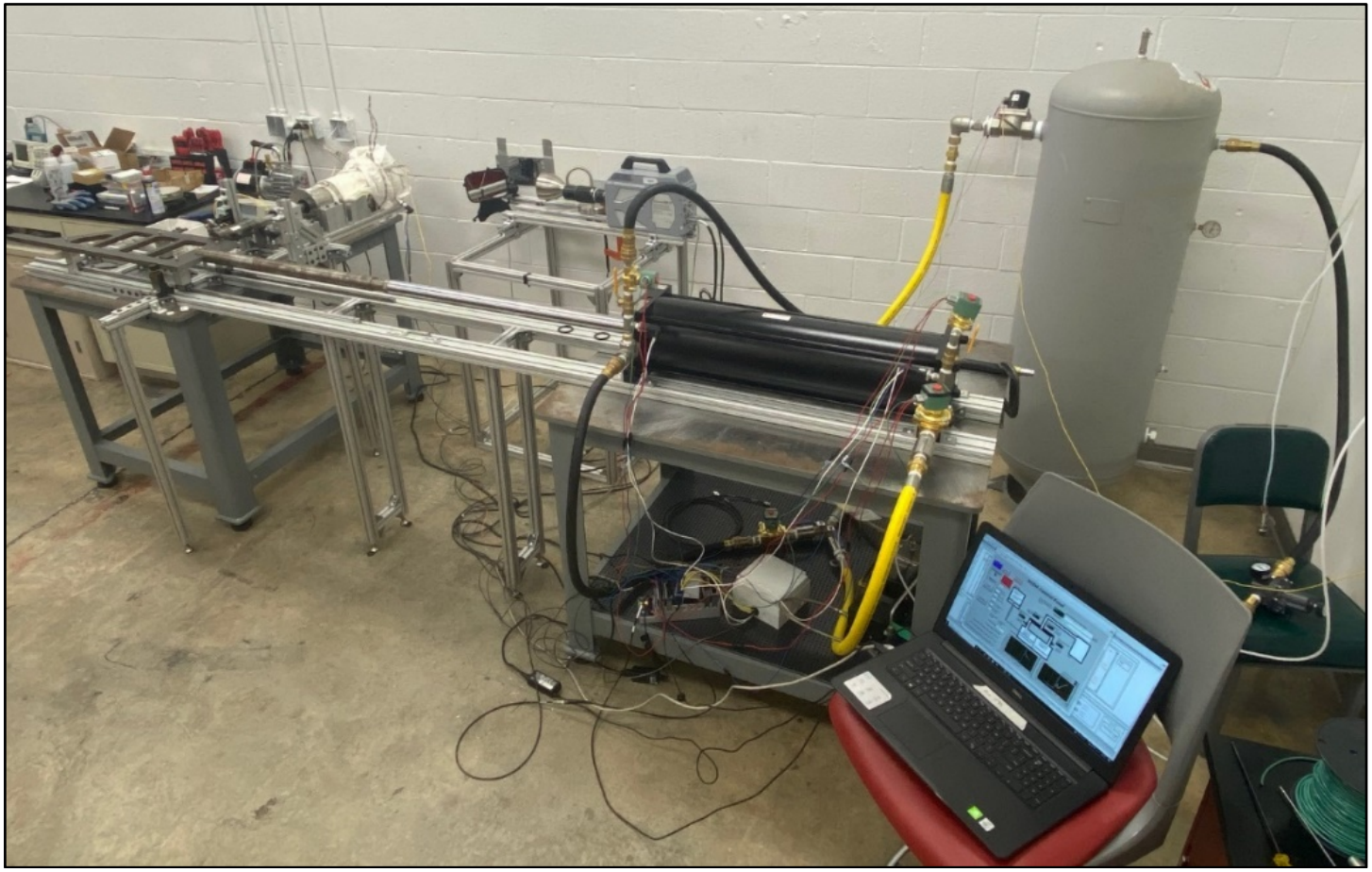

Figure 2.2: Final layout of rapid compression expansion machine (RCEM)

Figure 2.3: Image of one of the two tables used in the assembly of the RCEM [8]

Figure 2.4: First linear cam utilized on the RCEM in this research

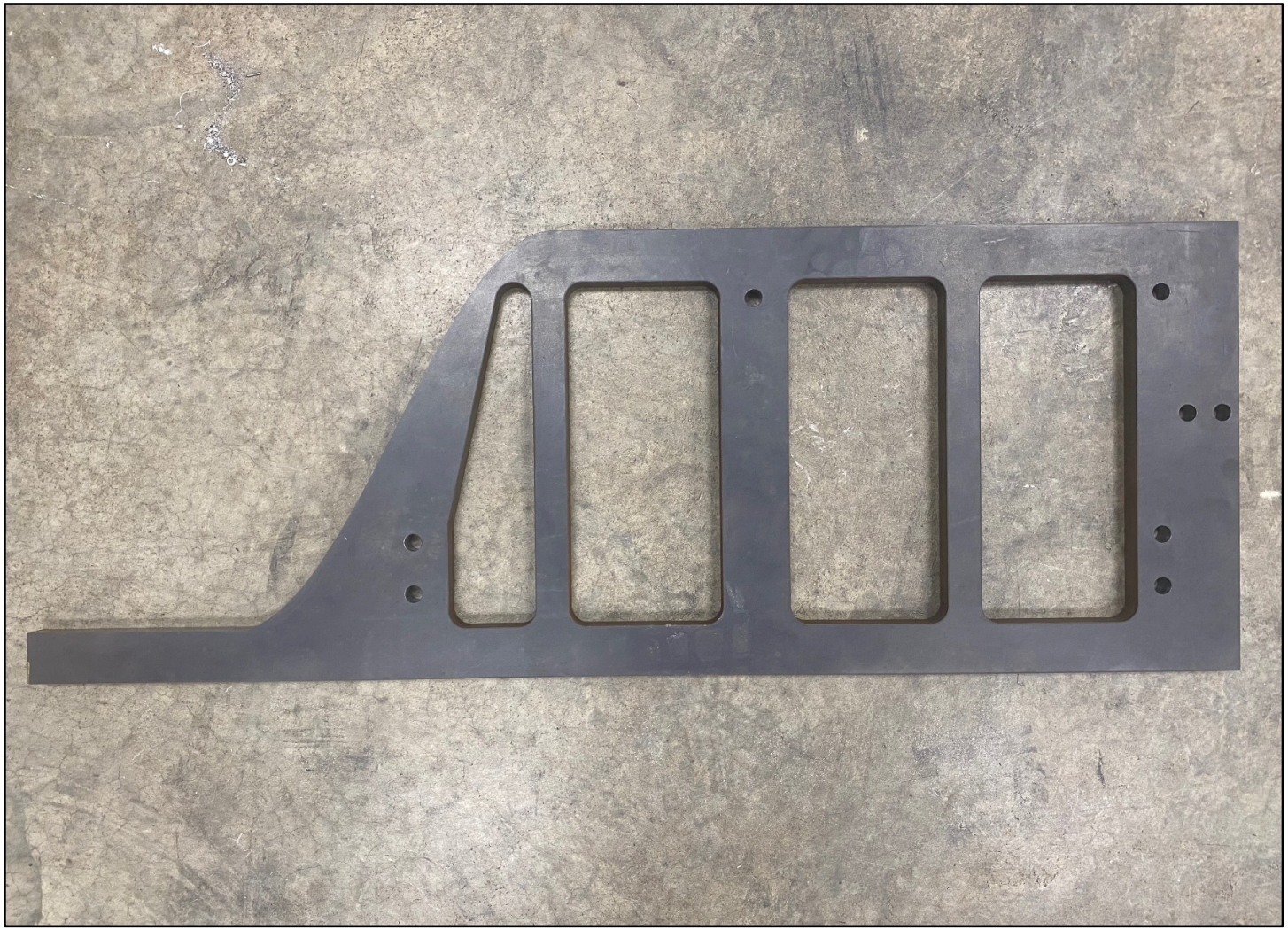

Figure 2.5: Second linear cam used on the RCEM in this research

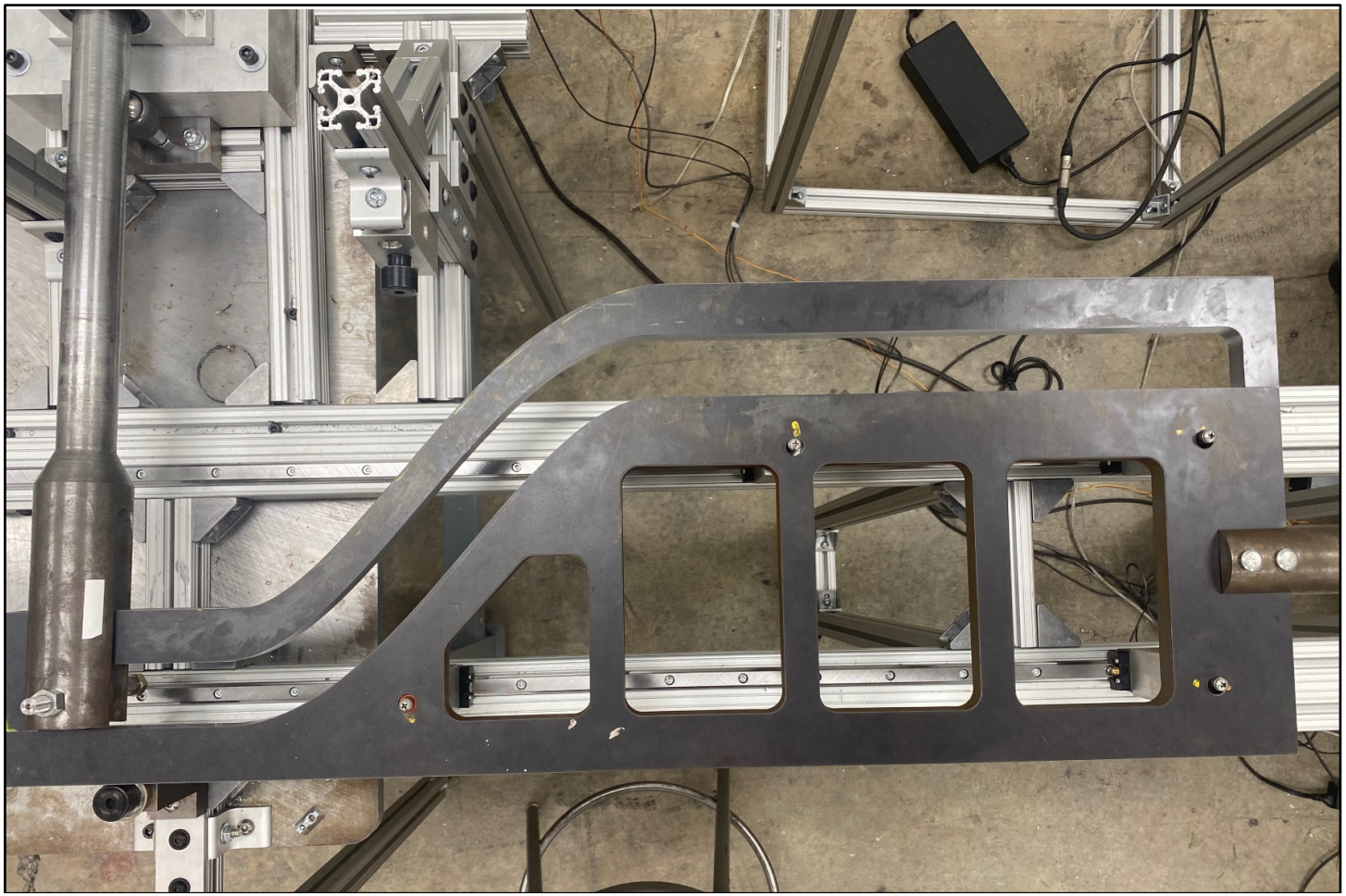

Figure 2.6: Third linear cam used on the RCEM in this research mounted on device

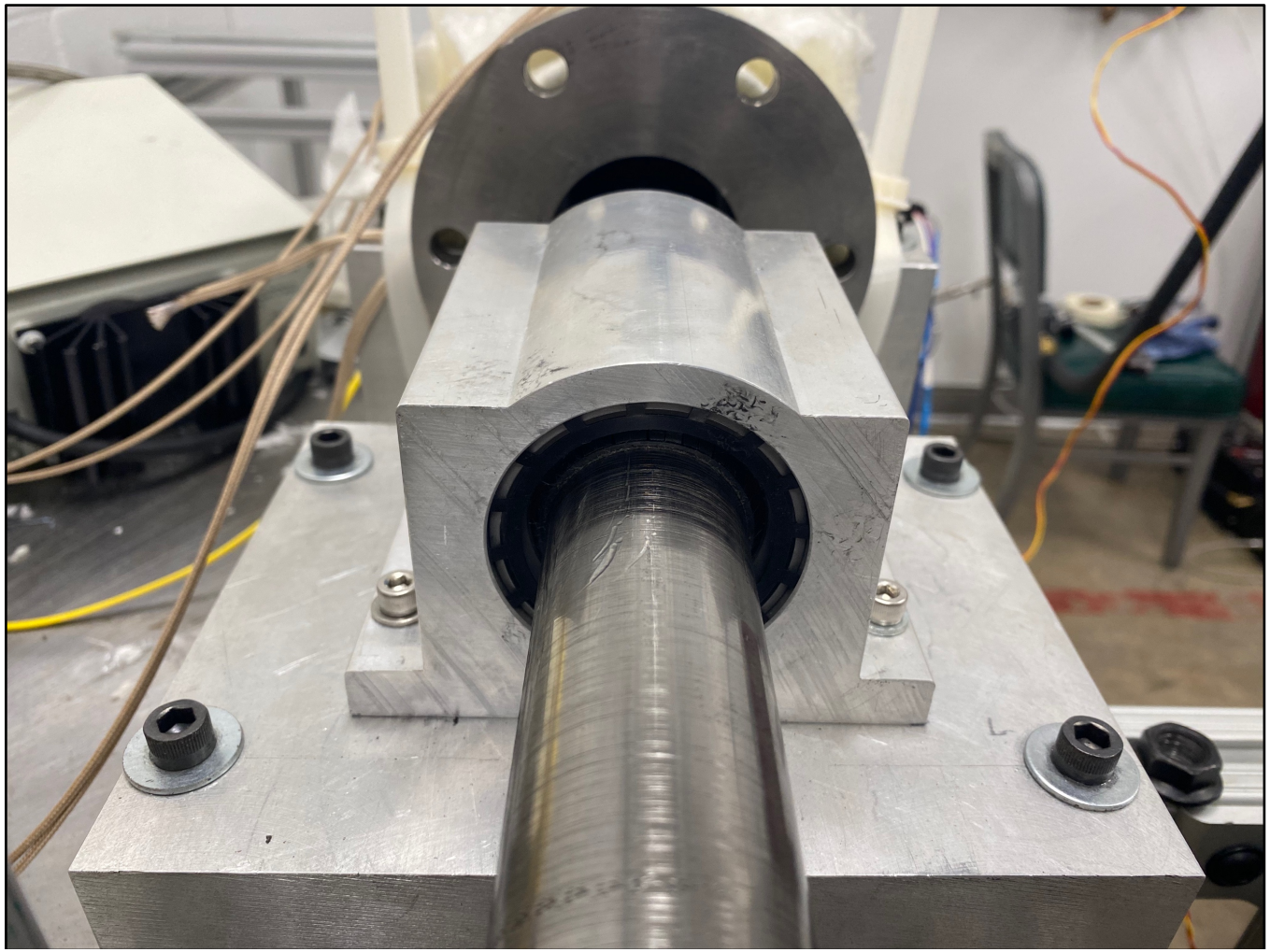

Figure 2.7: High load mounted linear ball bearing installed on RCEM

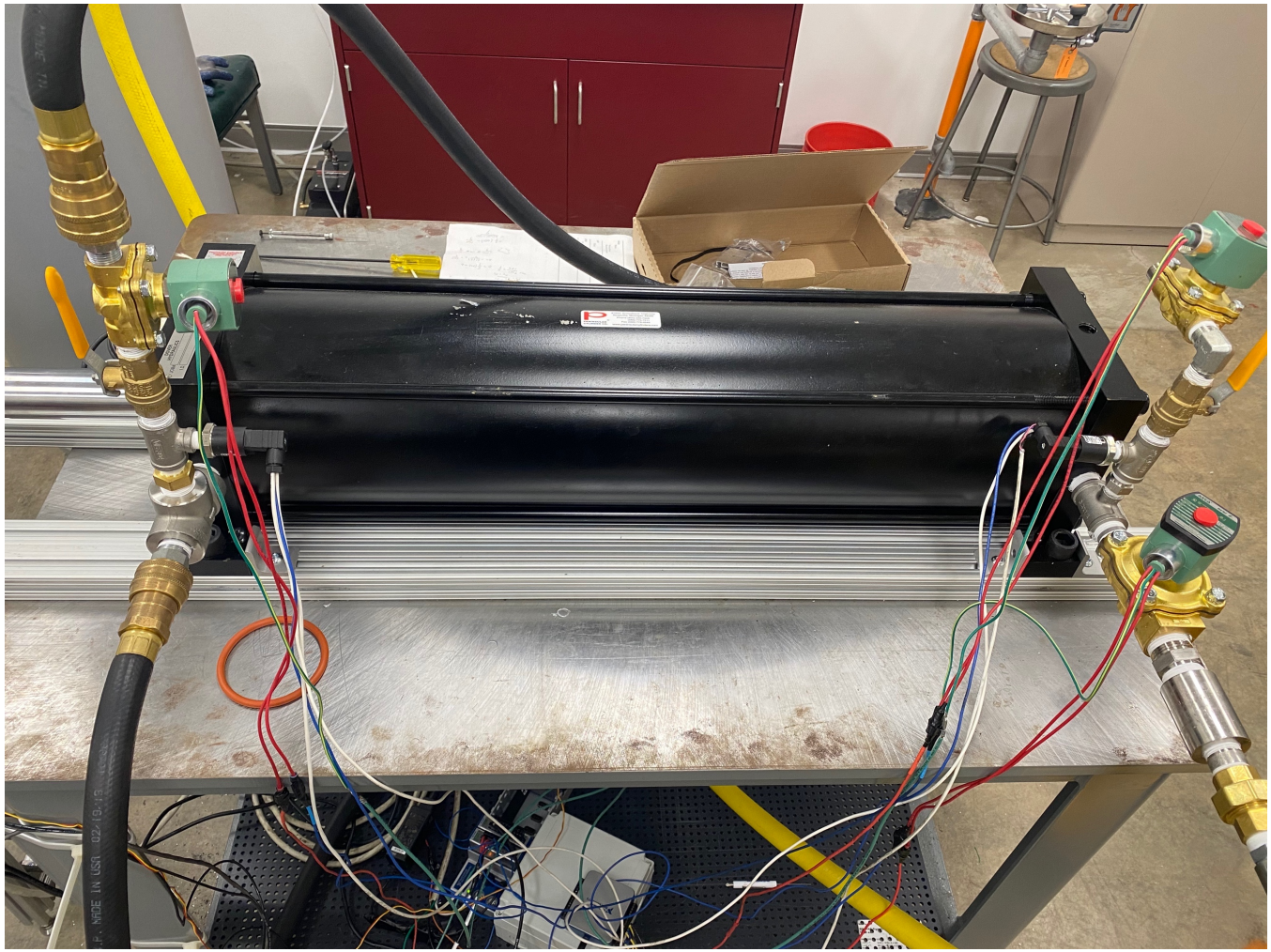

Figure 2.8: Custom pneumatic actuator, supplied by Dover Hydraulics, installed on RCEM

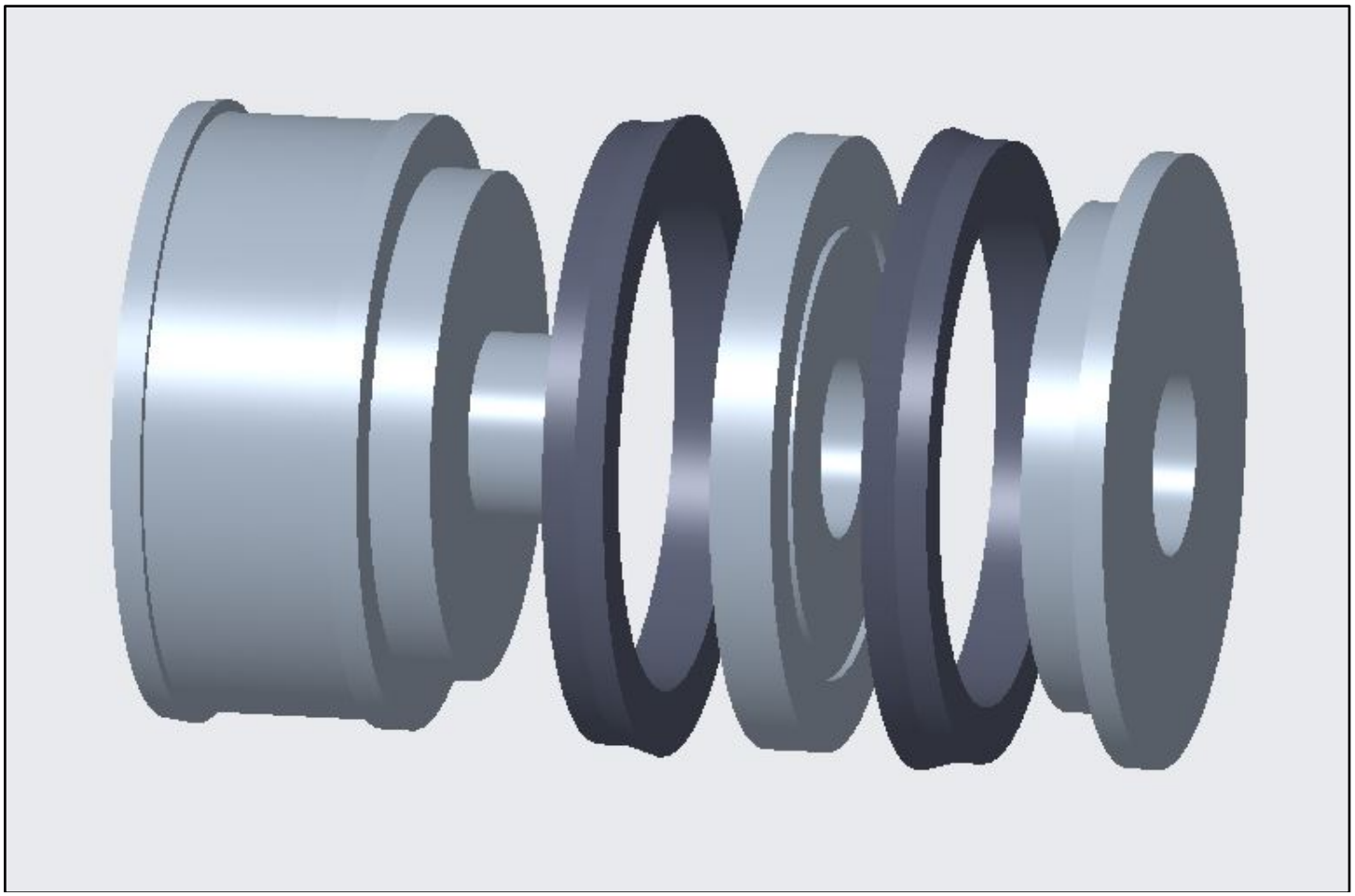

Figure 2.9: Exploded view of piston assembly

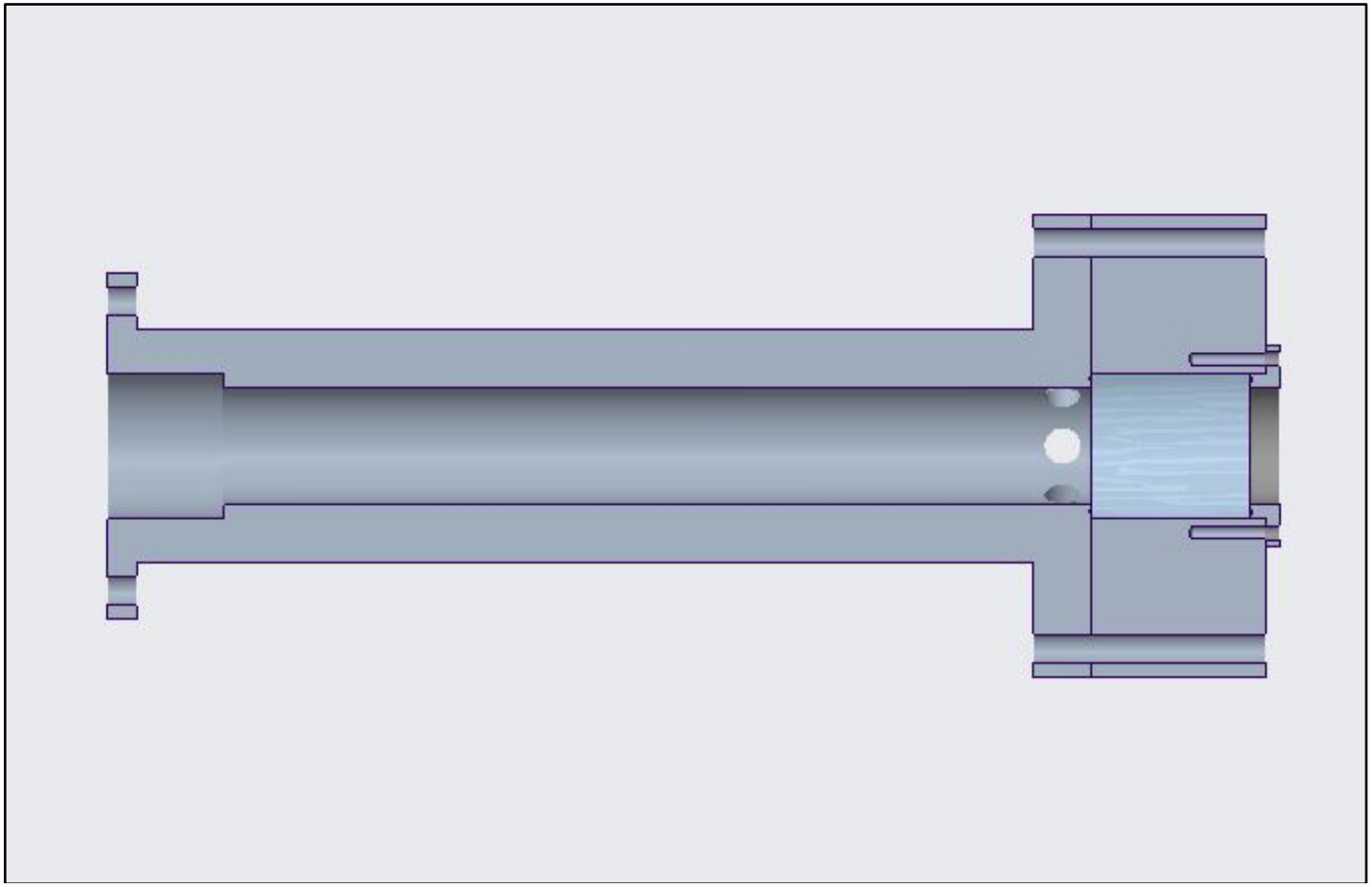

Figure 2.10: Schematic of the RCEM's cylinder/combustion chamber

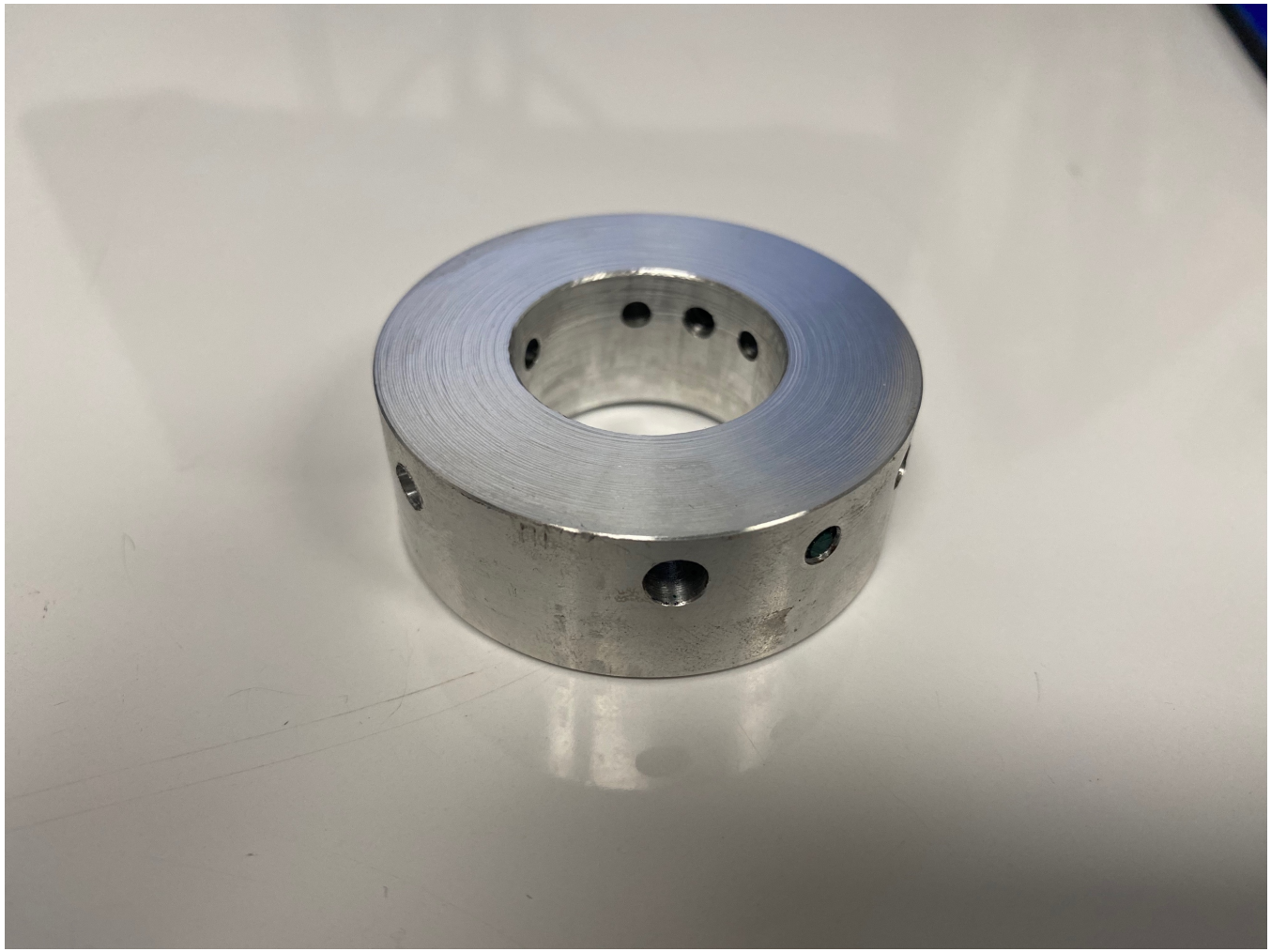

Figure 2.11: Stainless steel cylinder insert for volume reduction

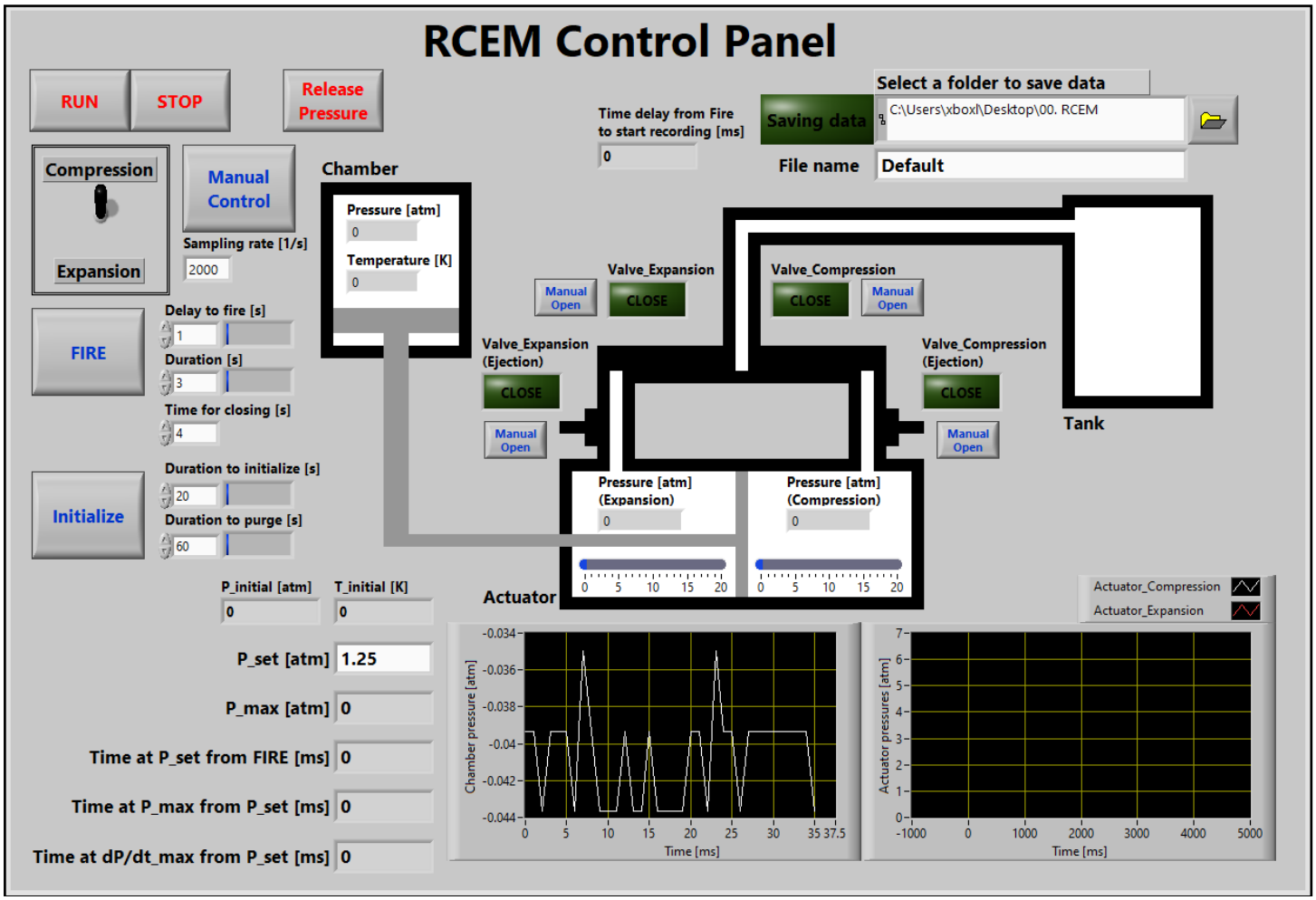


Figure 2.12: LabView user interface for the RCEM

# CHAPTER 3

## ASSEMBLY AND PERFORMANCE VERIFICATION

Since the machine is comprised of two separate tables joined by two pieces of double aluminum extrusion, the first parameter that needs to be checked is that the tables are parallel to each other. The tables were moved into their rough positions using a crane and were then adjusted using pallet jacks. It is critical that the tables are aligned to prevent any unnecessary stress on other components of the device. This alignment was done by measuring the distance from the edge of one table to the edge of the other table in the normal direction. This measurement was repeated at multiple points along the surfaces of the tables and adjustments were made accordingly with the pallet jack to ensure equal distances from each other. After this alignment was completed, the tables had to be leveled. The flat top tables still needed to be leveled because the floor in which they rest on is not as precise as the tables are. Leveling was done by adjusting three of the four extreme-force vibration-damping leveling mounts that were attached to the feet of the table. By using one foot as a pivot point, the other three feet were adjusted and checked with a bubble level to ensure that they were flat. After each table was leveled, the height of the tables had to be adjusted to make sure that the top surfaces were on the same plane as each other. This was done by adjusting all four feet on the table by the same amount. Once this was done, the tables were checked again to ensure that they remained level through the height adjustment.

The tables were then connected together by two 1-1/2” x 3” double slot aluminum extrusions which were made parallel with each other by connecting four 5.5” single slot

aluminum extrusions between them with gusseted corner brackets. This ladder-like extrusion assembly was created to ensure the actuator was in line with the cam guide rails. Once completed, the extrusion assembly was placed on top of the tables, so that both ends were flush with the far edges of each table. When the position was correct the extrusion was clamped to the table using various c-clamps so that holes could be drilled through both the extrusion and the tables using a magnetic base drill press. The magnetic base drill press was crucial to the assembly of this device because it allowed for holes to be created straight in both vertical and horizontal applications. The extrusion and the tables were bolted together using eight 1/4”-20 x 3” bolts on each table. This created a rigid connection between the two tables that would allow for very little deflection under load.

The actuator was then mounted to the extrusion in a similar way to how the extrusion was mounted to the table. By placing the actuator on the extrusion in the desired position and marking the extrusion with a punch, hole placement could be made very precise. Removing the actuator from atop the extrusion allowed for holes to be drilled through the extrusion and the table once again. This time the holes were made much larger so that the 3/4"-10 x 4” bolts, that fit securely in the mounting feet of the actuator, could be attached to the table while resting on top of the extrusion. Having the actuator fully constrained on the table prevents unnecessary stress on the 4 ball bearing carriages that guide the cam by ensuring that everything remains linear.

After the actuator was mounted, the cam needed to be mounted to the actuator rod. To do this, 2 1600mm guide rails were connected to the double aluminum extrusions with t-slot inserts that allow the rail to be tightened onto the extrusion by compression. Since the extrusion was mounted parallel to each other, the guide rails are also parallel. The 4

ball bearing carriages were then slipped onto the rail and checked for smooth operation. The ball bearing carriages each have 4 M4 x 0.7mm mounting holes on them that were used to attach risers. These risers bring the cam up to a height that is on the same plane as the actuator rod and parallel with the table. At the top of each of the risers, a standoff is placed so that the cam can be attached.

Now that the cam is attached, the cylinder can be mounted to the other table. 2 single aluminum extrusions were attached to both the table and the double aluminum extrusion spaced 5.5 inches apart. Similar to the way the double aluminum extrusion was mounted, 2 5.5-inch single aluminum extrusions were placed in between the 2 main pieces of extrusion to form a ladder-like reinforcement. This was then bolted to the table with the same 5/16”-18 bolts that were used for mounting the double aluminum extrusion. To mount the cylinder to these extrusions, 2 aluminum blocks were made with a 4-inch diameter semicircle cutout at the top that the cylinder could rest in. These blocks each had 4 holes running through the entire thickness of the block so that they could be attached to the extrusion with t-slotted framing fastener nuts. Due to the amount of pressure being generated from the device, corner brackets were added in front of the aluminum blocks because the compression of the block with the bolts and fastener nuts may not be sufficient to hold it in place. By adding these corner brackets, extra compressive force was added to prevent the cylinder from adjusting.

Once the assembly was completed and everything was aligned properly, the RCEM had to be tested for leaking once it was pressurized. To do this, the machine was fired, as it would be for running an experiment, with no fuel inside the cylinder. This allows the device to experience the same compression that it would see when operating. The pressure

transducer that is mounted to the cylinder can produce a live reading of the pressure within the LabView GUI. This is useful because the live reading can be monitored by the operator over any given amount of time to see if the compressed cylinder is leaking air.

In the first design of the RCEM, alignment and stress on components was a big problem. The compression ratio of the machine in the original configuration was designed to be 10:1 assuming that there was no unaccounted-for volume, also known as dead volume, within the cylinder and the clearance height was 1 inch. After the machine was fired and the piston was at TDC, the pressure was found to be just above 5 atm, which is half of what was expected. After analyzing the assembly, the problems that were found were that there were dead volumes, which were later corrected, and that air was escaping past the u-cup seals. Initially, it was a bit of a mystery as to why air was getting past the u-cups, but after further investigation, two different things were causing the leak. First, there was a machining error within the cylinder and second, the connecting rod was experiencing too much of a deflection which was causing the u-cups to compress against the cylinder wall.

The machining imperfection was only found when the cylinder was compressed by hand and was found to be a small groove running around the circumference of the cylinder wall that was about halfway through the length of the cylinder. This imperfection occurred because the cylinder needed to be bored out from either end due to the length that was required. In doing this, the hole that was created on one side was just slightly misaligned with the hole from the other side. Without special equipment, which none of the machine shops in the area had, the groove could not be fully removed without increasing the bore diameter of the cylinder. However, the groove depth was greatly decreased by honing and

polishing the cylinder, which eliminated the problem of air escaping past the u-cups as they passed by the groove. The deflection was occurring when the machine was fired because the connecting rod was acting as a cantilever as the cam was applying a load to it.

Due to the lack of the bearing in the first design, the connecting rod had too large of a deflection which was leading to the u-cups compressing against the cylinder wall and causing increased friction within the piston assembly. This caused air to escape past the u-cup on the opposite side of where the compression was occurring, as well as, causing them to wear unevenly and decrease the ability of the piston to move freely. To fix this issue, a support was needed to keep the connecting rod from deflecting while still allowing it to move into the cylinder. A high load mounted linear ball bearing was selected as the best form of support for the connecting rod. This ball bearing had an extremely low degree of deflection at just 0.5 degrees. The bearing was mounted to the rails the cylinder was mounted to via a 4-inch-thick aluminum block. This ensured that the center of the bearing was concentric with the cylinder and that the u-cup seals would wear evenly and prevented leaks from occurring after a few runs.

As mentioned earlier, 3 different cam profiles were used in the development of this machine. The cam that was designed initially was used for most of the testing of the RCEM. The 9-inch stroke over 12 inches was providing a relatively smooth compression stroke over the entire range of actuation pressures. This was mostly due to the maximum angle of attack from the cam being around 50 degrees. The pressure profiles from the first cam, shown in figure 3.1, compare the cylinder pressures during a non-reactive experiment at multiple actuation pressures. This was done so that the compression time could be calculated and so that the peak pressure generated could be determined. The actuation

pressures that were tested ranged from 10 psi to 130 psi. To be able to read the figure more clearly, only 4 actuation pressures are displayed. The 50 psi and 80 psi curves show smooth compression as well as a decrease in compression time as the pressure is increased. To further decrease the compression time, the actuation pressure needed to be increased. At 100 psi, compression time was decreased, however the pressure curve develops a period in which compression slows down before increasing again. Initially, the reason for this occurrence was a mystery, but was eventually determined to be the roller jumping off the cam surface after a high-speed video was taken of the roller during the experiment (figure 3.2). The roller was detaching because the acceleration of the cam was producing a force greater than the force that the pressure in the cylinder was generating. This occurrence was seen in other RCEM designs that utilized an open profile cam [6]. Since the profile of the cam is sinusoidal, the inflection point will start to reduce the acceleration of the piston, assuming it stays attached. When the roller reached the inflection point, it detached from the cam, resulting in a decrease in acceleration greater than what was intended before reattaching and continuing the compression stroke. At 130 psi, the pressure curve looks very different from the other pressure curves. Just like the 100-psi curve, the curve is not smooth and a decrease in compression time was seen. Detachment was also occurring at this pressure, which was expected, but the detachment was much greater than before. When this happened, the roller jumped high enough to cause the pressure in the cylinder to increase high enough to generate a force that was able to produce negative acceleration of the piston. When negative acceleration occurs, the piston is expanding instead of compressing. After it expands for a short period, it reattaches to the cam and begins to compress again as intended.

The expansion period on this cam, although not very apparent, is also a problem. The pressure drop after the piston reaches TDC is too rapid. The problem with this is that the pressure directly correlates to the temperature in the cylinder. If the pressure drops too rapidly in the cylinder, then the temperature will too. This is a problem mostly for tethered droplet ignition. For the droplet to ignite, some of the fuel must first evaporate. If some of the fuel evaporates, but the temperature in the cylinder drops before it can ignite, then ignition will not occur. Even with no expansion period in the cam, the pressure will still drop due to heat loss to the environment, but the time in which heat loss occurs can be reduced.

The first cam worked well enough to collect some initial data, but there were several problems that could be improved upon. The main problems that were preventing the RCEM from achieving repeatable, combustion conditions were the roller jumping and the expansion period. To try to fix these problems, a second cam was designed.

The second cam aimed to fix some of the issues with the first cam. To do this, a double harmonic curve was used to decrease the initial acceleration and to increase the acceleration later in the compression stroke. The stoke for this cam was also increased from 9 inches to 11 inches to further increase the compression ratio in the RCEM. Doing this allowed for higher final pressures to be achieved because the starting volume was increased while maintaining the final volume. In addition to the stroke being increased, the compression time was decreased. This was done by decreasing the distance in which the stroke occurred. The period of compression was decreased from 12 inches to 8 inches. In theory, if the cam's velocity remains the same for a given pressure as it did with the first cam, then the compression time would be reduced by 25%.

This new cam did not behave as intended and resulted in more work instead of fixing issues. Since the cam profile was different, the maximum angle of attack on the roller was increased from 50 degrees to nearly 70 degrees. This was known before testing began and was a bit of a concern, so in an attempt to reduce damage if the cam was too aggressive, actuation pressure was reduced to 10 psi and would gradually be increased in increments of 10 psi. At 10 psi, the pressure curve is drastically different from the pressure curves displayed with the first cam. There was a large studder in acceleration of the piston which was caused by the cams aggressive profile. At 20 psi, the curve becomes much more like the curves seen previously, but there was still a very slight studder in the compression. Moving to 30 psi, the pressure begins to smooth, and no stuttering can be seen. A trend of decreased compression time can also be seen as the pressure increased, which was to be expected. At 40 psi, no studder is seen again and the compression time was further decreased. The RCEM seemed to run smoother as the actuation pressure was increased with the second cam attached. When the pressure was increased again is when the machine failed. At 50 psi, the lateral force being applied to the connecting rod was too great and resulted in the shearing of 4 of the cylinders mounting bolts as well as the deformation of the 4 linear bearing mounting bolts. All 5 of these pressure curves can be seen in figure 3.3.

To try to fix the second cam, the roller surface was reprofiled to a simple harmonic curve that increased the compression period from 8 inches to 9.5 inches. A comparison of the reprofiled cam structure compared to the original can be seen in figure 3.4. This reduced the angle of attack from 70 degrees to 66 degrees. After testing this cam, the same stuttering

was still occurring at low pressures and the linear bearing mounting bolts were still bending. The second cam needed to be removed and a new cam needed to be designed.

The third and final cam utilized on the RCEM was a hybrid of the first 2 cams with most of its design drawing similarity from the first cam, but also included some new features. The new cam has the same stroke and compression periods of 9 inches and 12 inches respectively, as seen in the first cam. The machining processes used, as well as the lack of an expansion period were taken from the second cam. The new feature added to the cam was a roller holder which was designed to prevent the roller from jumping off the cam at the inflection point of the curve. So that the roller could still roll, and not slide along the profile, a .02-inch gap was included. Since the compression stroke was reduced, the only other way to increase the compression ratio was to adjust the cylinders position so that both the initial and final volumes are decreased. If this wasn't done, the compression ratio would have been the same as the first cam in the cases where the roller did not jump off the cam. The clearance height was adjusted from about 1 inch to about 0.7 inches. Since dead volumes are still present, even though greatly reduced, the compression ratio would not have been the calculated 13.9:1, but with the inclusion of the metal insert mentioned before, the compression ratio was measured to be 14.4:1. The compression ratio can be measured in two different ways. The first is to isothermally compress the piston, which can only be done by hand. This is a challenge at high compression ratios because it is difficult to generate enough force to move the piston up to TDC. The second method is to compress it at full speed and wait for the temperature to return to initial conditions. Doing this method revealed that the compression ratio was 14.4:1. The compression ratio is not to be confused with the peak pressure. The faster the piston compresses, the higher the peak pressure

would be. Since the roller is limited to actuator pressures under 140 psi, the quickest the piston could accelerate was at an actuation pressure of 130 psi. Measuring the peak pressure from the experiment is simple because the LabView code is set up to record and display the highest pressure that was experienced. With the third cam, the peak pressure was measured to be 28.6 atm.

The same compression testing that was done with the first two cams was also done with the third cam, but this time from 20 psi to 120 psi. Figure 3.5 shows 4 of the pressure curves from these tests. Comparing these pressure curves to the ones seen in figure 3.1, it can be seen that a drastic improvement was made with controlling the jumping of the roller. The 50, 80 and 100 psi curves show a smooth pressure profile with no visible stuttering or roller jumping. The 120-psi curve shows no stuttering, but it does show a very slight jump of the roller. This is still to be expected because of the 0.02-inch tolerance included with the roller holder, which will still allow to roller to jump, but it is extremely limited in the distance it can leave the cam surface.

Analyzing the data from the compression testing allows for multiple figures to be generated that help show the improvements that have been made. Figure 3.6 shows that as the pressure delivered to the actuator increases, the compression time decreases. Using this compression time data, a power trendline was generated that allows for estimations of compression time for different actuation pressures. The n value is important because it shows how close to isentropic the compression is. A n value of 1.4 is isentropic for air. It can be seen from this data that as the compression time decreases, the n value increases. The n value can also be used to estimate the temperature. The estimated temperature data is shown in figure 3.7 and it shows that the temperature increases as the actuation pressure

is increased. This is useful because it can help determine if a fuel that is going to be used in an experiment will begin to vaporize.

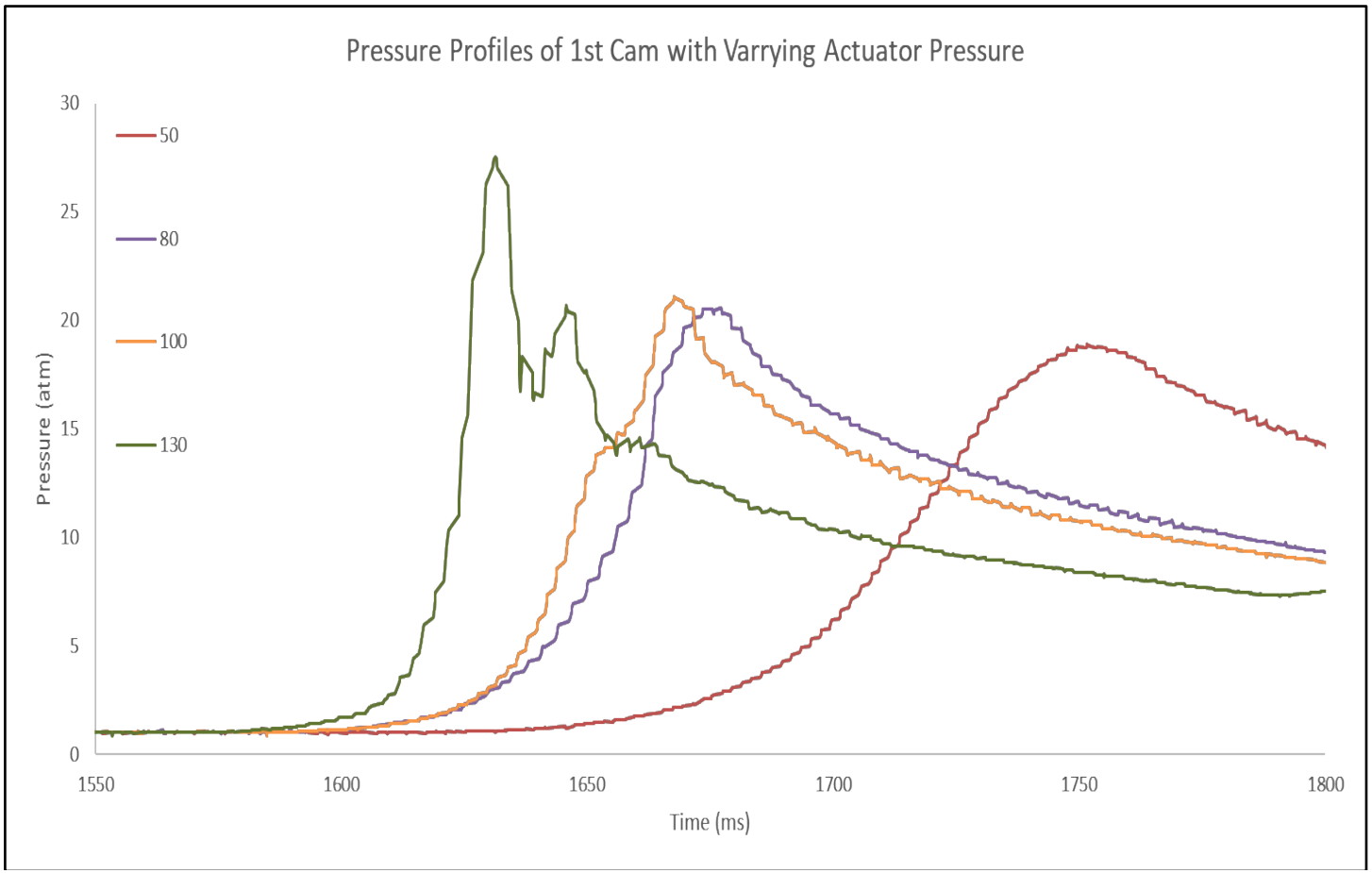


Figure 3.1: Pressure profile comparison of 1st cam with varying actuator pressures

Figure 3.2: Frame from high-speed video that shows maximum roller detachment

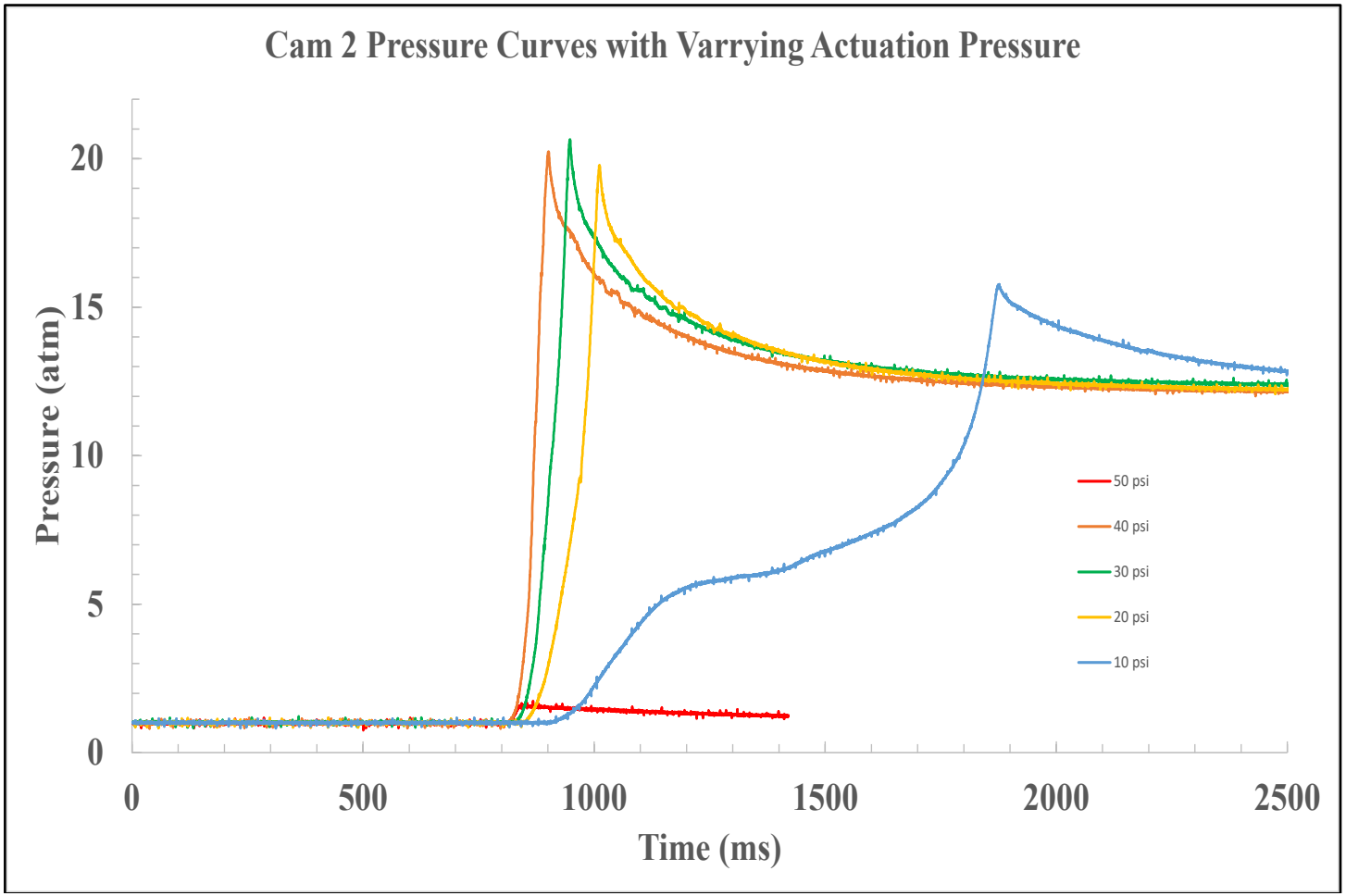


Figure 3.3: Pressure profile comparison of 2nd cam with varying actuator pressures

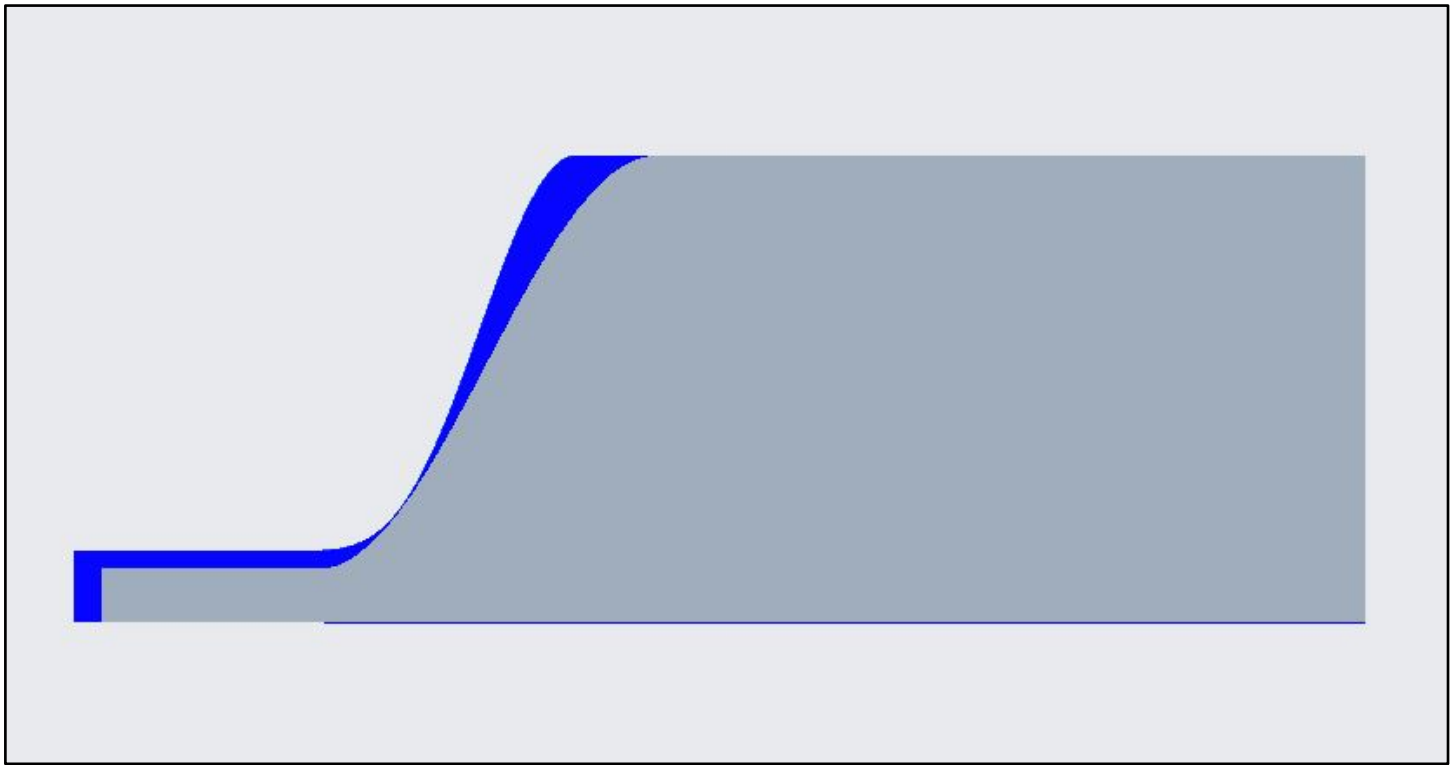

Figure 3.4: Assembly showing a comparison of the 2nd cam's modifications

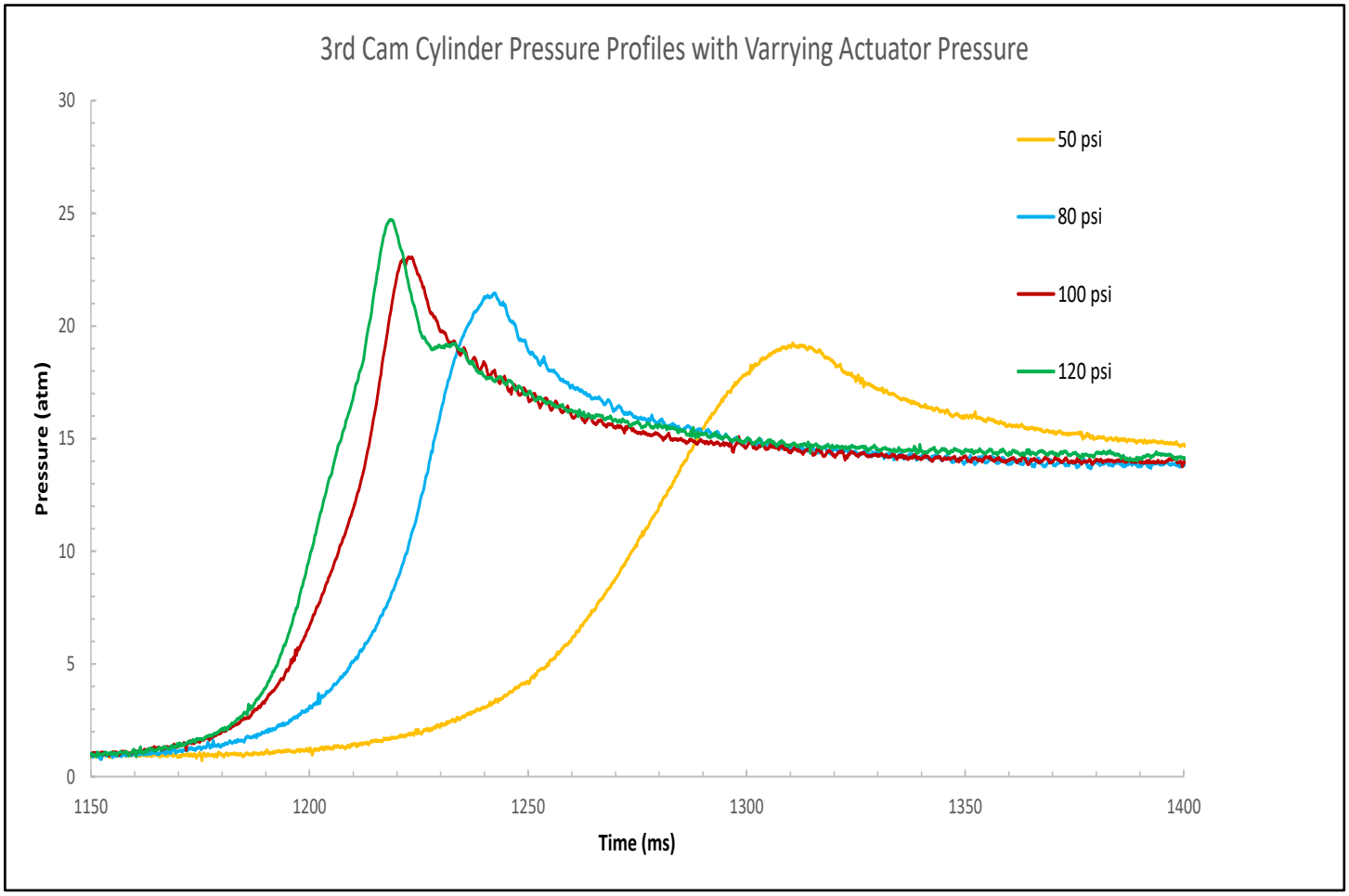


Figure 3.5: Pressure profile comparison of 3rd cam with varying actuator pressures

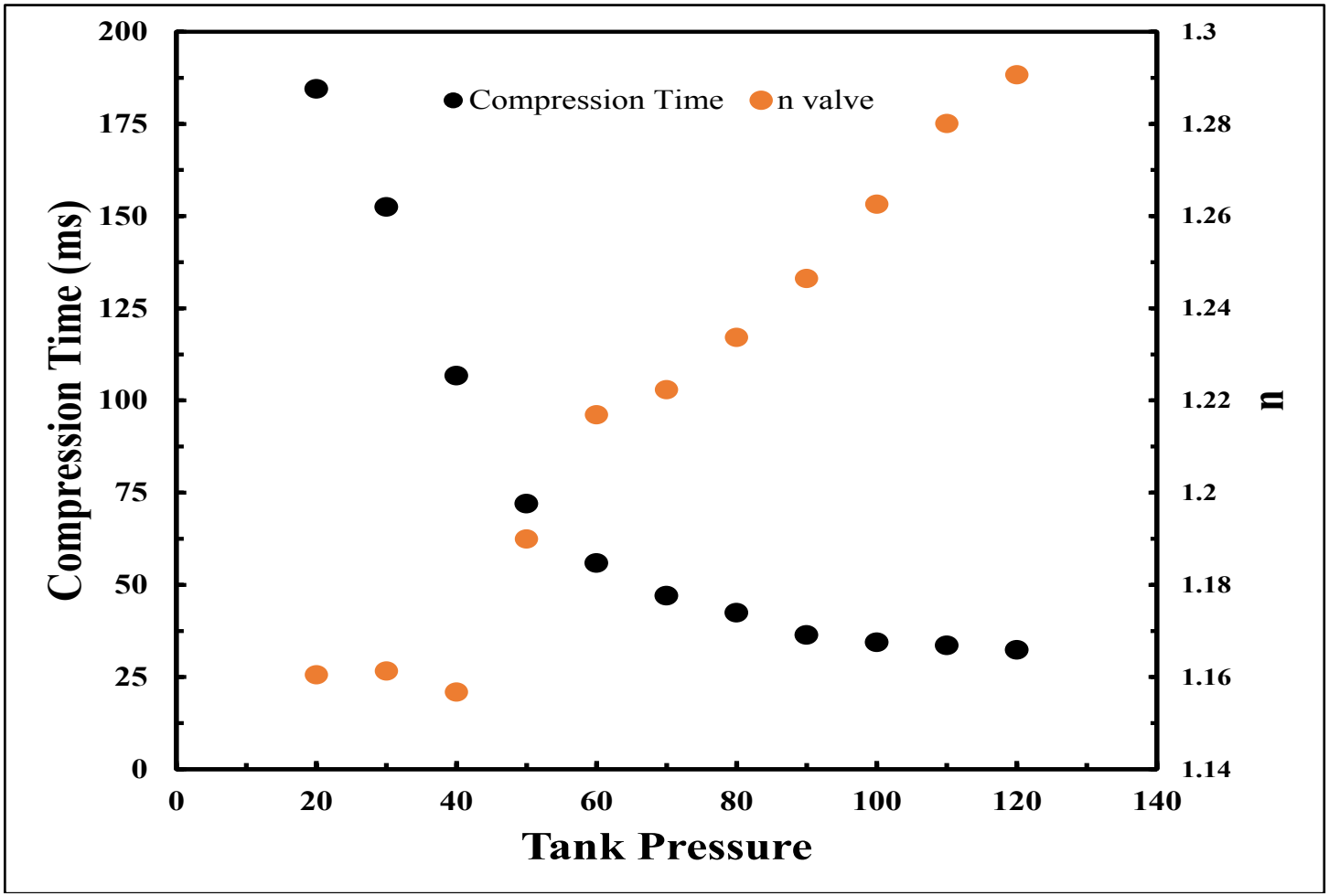


Figure 3.6: Compression time and n-value vs tank pressure for the 3rd cam

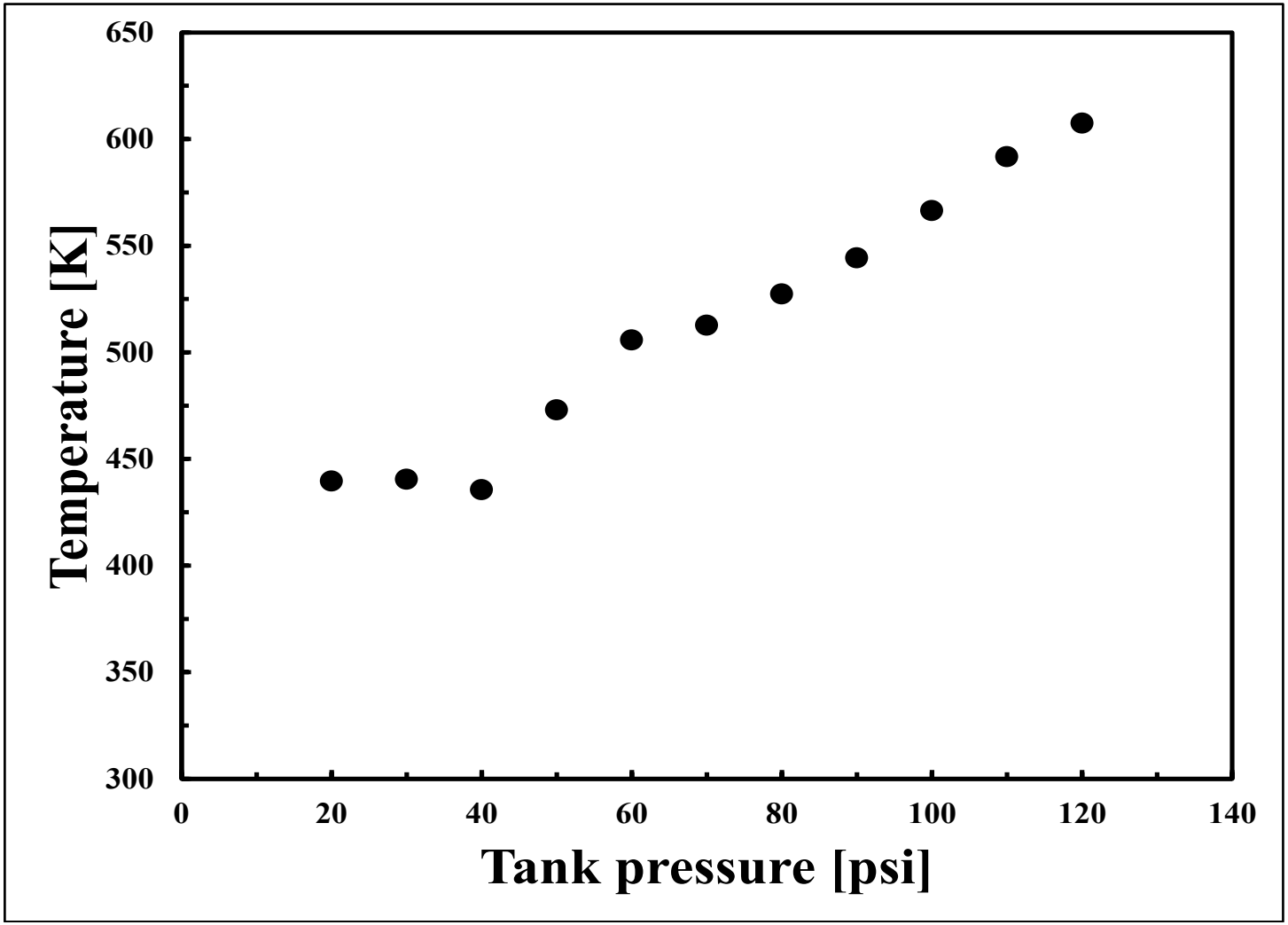


Figure 3.7: Estimated temperature vs tank pressure for the 3rd cam

# CHAPTER 4

# EXPERIMENTAL RESULTS

Now that the RCEM has been verified to produce repeatable compression data, reactive experiments can now be performed. The two types of experiments done in this research were homogenous charge compression ignition and tethered droplet ignition. To do these experiments, a couple of changes were made to the RCEM. The metal plate being used as a placeholder during the compression testing was swapped out for a glass window. Additionally, the high-speed camera and a mirror were added to view the inside of the combustion chamber during the experiments. These experiments are important because they help analyze ignition behaviors that occur in the real world. The data from these experiments can be used to help improve engine performance.

## HOMOGENOUS CHARGE COMPRESSION IGNITION

Homogenous charge compression ignition, or HCCI (shown in figure 4.1), is an experiment that combines the characteristics of gasoline and diesel engines. Gasoline engines use homogenous charge spark ignition, or HCSI (shown if figure 4.2), while modern diesel engines utilizing direct injection use stratified charge compression ignition, or SCCI (shown in figure 4.3). Like a gasoline engine, fuel is injected into the cylinder before compression where it mixes with air, but instead of using a spark to ignite a portion of the mixture, the air/fuel mixture is compressed to a point where the temperature causes autoignition.

With the RCEM, HCCI was first attempted by injecting a small, measured amount of fuel into the cylinder via a syringe at the top instrumentation port of the cylinder head and sealing it with a plug. In this first attempt, the cylinder was at BDC and there was no heating of the cylinder. With these conditions, a single component fuel with a low vaporization temperature needed to be chosen. The first fuel that was used was n-Heptane because of its relatively low vaporization temperature of 98.4 degrees Celsius and good reactivity [13]. Once injected, a timer was set for 5 minutes to allow the fuel to vaporize and mix with the air. After the 5 minutes, the RCEM was fired, and the data was recorded.

First, looking at the pressure data, there was no visible difference in pressure. If ignition occurred there should have been a pressure increase. Just in case there was an issue with the pressure sensor, the high-speed video was analyzed frame by frame to see if any kind of ignition occurred. After looking at the video it was confirmed that ignition did not occur in this experiment. The fuel most likely did not fully vaporize or mix well within the cylinder. To fix this a new method for injecting the fuel had to be used.

By looking at how fuel is injected in a HCSI engine, which is port injection, a new method was developed. To do this, the piston needed to start at TDC, and the cylinder needed to be heated to 100 degrees Celsius. With the top instrumentation port open to the atmosphere, fuel will be injected as the machine is initialized. As the piston is returning to BDC, air is rushing into the top instrumentation port as the fuel is being injected. This acts just like the intake stroke of a 4 stroke, HCSI engine, where the intake valve opens as the piston is moving from TDC to BDC and the air/fuel mixture enters the cylinder. Once the fuel was injected and the piston returned to BDC, the top instrumentation port was capped, and the experiment was ready to begin.

With this new injection method, n-Heptane was put into a syringe and its mass was measured. After the fuel was injected, the syringe's mass was measured again to determine the amount of fuel used. The amounts of fuel injected varied from 17.12 mg to 101.8 mg, giving equivalence ratios varying from 0.52 to 3.29, where 0.52 is a very lean mixture and 3.29 is a very rich mixture. The equivalence ratios that were focused on were the very lean, very rich and stoichiometric conditions. Starting with the very rich mixture, the experiment was run, and combustion occurred. The images, shown in figures 4.4-4.6, show three frames from the high-speed video taken during the experiment. The first frame, shown in figure 4.4, is when the piston reaches TDC, just before ignition occurs. The frame displayed in figure 4.5 is right when ignition occurs. The final frame is several ms after ignition occurs, which can be seen in figure 4.6. Ignition occurred just after the piston reached TDC and the delay of ignition from the firing of the device was measured to be 192.5 ms. The stoichiometric condition utilized 33.76 mg of n-Heptane, which had an equivalence ratio of 1.04. The three frames shown from this equivalence ratio, seen in figures 4.7-4.9, are at the same points as the rich mixture, where figure 4.7 is just before ignition, figure 4.8 is right at ignition, and figure 4.9 is just after ignition. Ignition occurred just after TDC again but had a reduced delay from the firing of the device at 182.5 ms. The very lean condition used the least amount of fuel at just 17.12 mg. The three frames from this lean condition experiment can be seen in figures 4.10-4.12. Just like the rich and stoichiometric mixtures, figure 4.10 is just before ignition, figure 4.11 is right when ignition occurs, and figure 4.12 is a few ms after ignition. The delay from fire to ignition was the shortest at 180 ms for this mixture.

The pressure curves for the 3 equivalence ratios discussed are compared in figure 4.13. The lean condition, shown in green, has the lowest increase in pressure of the 3 different curves. This makes sense because there was the least amount of fuel to react. The stoichiometric and rich equivalence ratio pressure curves, shown in blue and red respectively, have peak pressures above what the pressure transducer used at the time was capable of reading, which is why they both have plateaus. By looking at the data that was recorded, it can be inferred that the peak pressure for the rich mixture was higher than the stoichiometric peak pressure because of the presence of one plateau as opposed to two. The data from these two curves is still useful though because the ignition delay difference between the two curves can still be seen.

The HCCI experiments were a success because they showed that autoignition could occur for n-Heptane. Since n-Heptane is a light and volatile molecule that is present in many fuels, the ability to experiment with it in real world conditions allows for a better understanding of how it affects real fuels. In real fuels, the presence of lighter hydrocarbons may have an effect on the whole fuel's ignition properties due to the effect of preferential vaporization. If the lighter molecules vaporize before heavier molecules, due to the temperature not being high enough, knock and low speed pre ignition can occur, which can be detrimental to the engine. Using the information gathered from this experiment and applying it in other experiments will allow for the exploration of how preferential vaporization effects overall ignition.

### TETHERED DROPLET IGNITION

To better understand the effects of preferential vaporization, multiphase ignition needs to be explored. Multiphase ignition occurs when partially vaporized fuel ignites. This

can occur when liquid fuel is sprayed into an engine from an injector. Although this phenomenon can occur in port injection, it is more likely to occur in direct injection. For example, modern SCCI diesel engines, which utilize direct injection, spray fuel from the injector straight into the cylinder. Depending on the compression ratio and how compressed the air within the cylinder is at the time of injection, the fuel may not fully vaporize due to the temperature not being high enough. However, some components of the fuel may vaporize and ignite before other components. The ignition of these components would then increase the temperature in the cylinder and the rest of the fuel would start to vaporize and ignite. The delayed ignition of the rest of the fuel can also result in reduced efficiency because the piston may already begin its expansion stroke which would result in less work being generated.

To experimentally look at multiphase ignition in the RCEM, a droplet tether was added to the cylinder head at the top instrumentation port. The droplet tether consists of a 1/8-inch outer diameter tube with an inner diameter of 0.027 inches in which a 0.006-inch diameter stainless steel wire is inserted into and epoxied. This allows for a droplet to be manually tethered outside of the cylinder and then placed inside so that it is suspended at the center of the window, seen in figure 4.14. Since the cylinder is being heated with heating tape to 100 degrees Celsius, a lighter fuel like n-Heptane can no longer be used because it will vaporize immediately. The fuel used in this experiment was n-Dodecane due to its heavier molecular weight, good reactivity, and higher vaporization temperature of 215.9 degrees Celsius [14].

To begin the experiment, the RCEM is reset so that the piston is at BDC, and the droplet tether is removed from the cylinder. This ensures that the cylinder is at atmospheric

pressure after the cylinder has been heated. A syringe filled with n-Dodecane is then used to create a small droplet that can be transferred to the tether. Given the surface area of the stainless-steel wire and the surface tension of n-Dodecane, the droplet size is limited to about 1 mm. If the droplet is any larger, it will not be able to overcome the force of gravity and it will fall off of the tether. Once the droplet is tethered, it is carefully inserted into the top instrumentation port and is secured via a compression fitting at the other end of the tether. After inserting the droplet, confirmation that the droplet is required because of the tight tolerances within the instrumentation port. By looking through the window at the cylinder head with a light, the droplet can be seen. If it is no longer there, then the cylinder needs to be vacuumed so that the fuel can vaporize and exit. When the droplet is successfully placed within the cylinder and the compression fitting is secured, the RCEM is ready to fire.

With just n-Dodecane tethered to the droplet, ignition proved to be quite difficult because the increased temperature from compression is only experienced for a very short period of time. The vaporization temperature of n-Dodecane is about 216 degrees Celsius which is 116 degrees higher than the temperature within the cylinder. Some of the fuel is still vaporizing, but not enough to achieve a localized equivalence ratio that can ignite. To allow for ignition to occur, changes needed to be made to the experiment. Since a larger droplet can't be used, n-Heptane was directly injected into the cylinder while the piston was at BDC, the n-Dodecane droplet was inserted, and the RCEM was ready to fire. Doing this simulated the vaporization of the lighter components within a fuel during the compression stroke. It should be noted that the ignition of the n-Heptane will not behave like it did in the HCCI experiment because a small amount of fuel was used to create a

small pocket in which the equivalence ratio is rich, but because of the overall amount of air in the cylinder, there will still oxygen remaining for the droplet to ignite. The first frame, shown in figure 4.15, is the ignition of the directly injected n-Heptane's vapor which was localized to the bottom of the cylinder. The second frame, which can be seen in figure 4.16, shows the ignition of the tethered droplet due to the increased temperature from the other ignition. When the temperature increased from the first ignition, the droplet began to vaporize at a much quicker rate than if the first ignition did not occur. With the increased vaporization rate, enough fuel evaporated to ignite. While the vapor around the droplet is ignited, the remaining liquid n-Dodecane continues to evaporate and ignite until it is depleted. The complete depletion of the droplet may only be possible because the cam being utilized does not have an expansion period, which keeps the temperature higher longer. If expansion was included in this cam, the flame may extinguish with some liquid n-Dodecane remaining.

The pressure profile from this experiment compared to a non-reactive compression, figure 4.17, reveals that the pressure rise is not nearly as large as it was with HCCI. The tethered n-Dodecane droplet ignition pressure curve, shown in blue, has a nearly identical pressure profile shape to the non-reactive pressure curve shown in orange. The only real difference between the two curves appears to be that the magnitude of the droplet ignition pressure curve is greater than the non-reactive pressure curve. This shows that the resulting ignition from the incomplete vaporization of a fuel produces a lower peak pressure than the peak pressure from the lean conditions in the HCCI experiment.

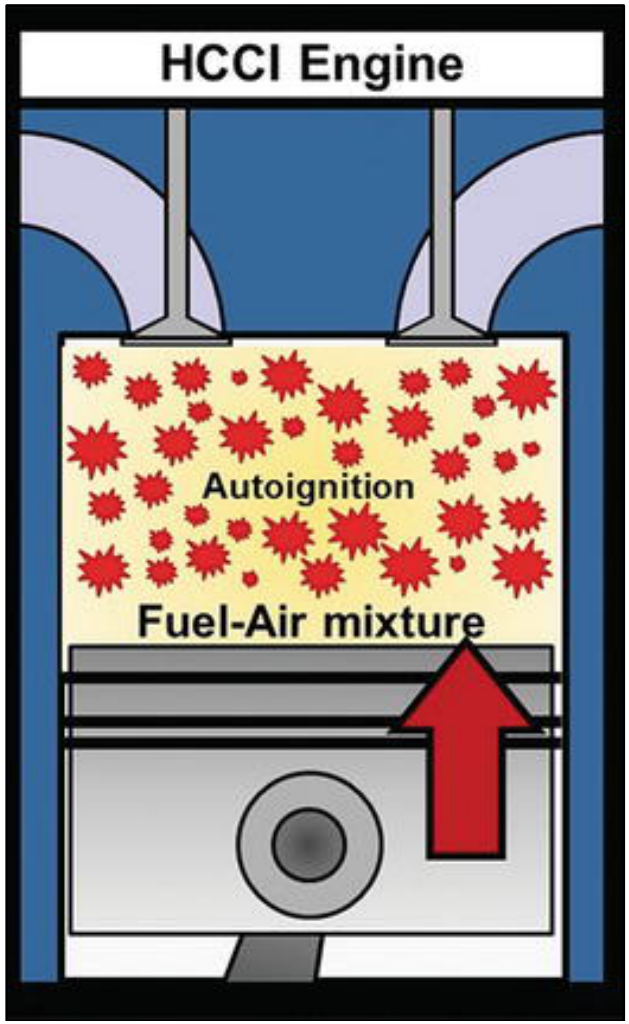


Figure 4.1: Diagram of homogenous charge compression ignition (HCCI) [12]

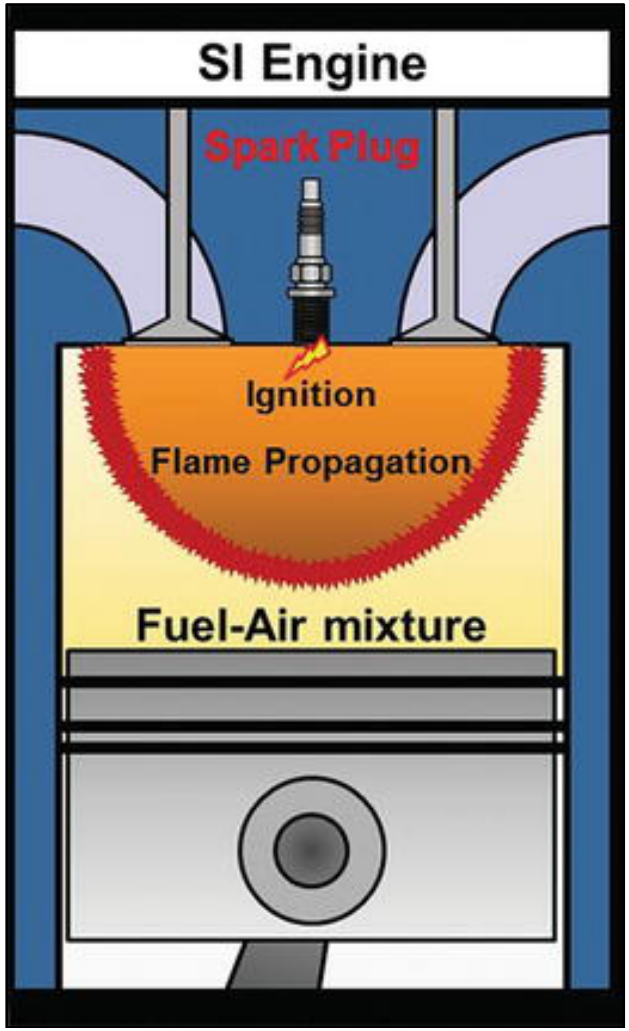


Figure 4.2: Diagram of homogenous charge spark ignition (HCSI) [12]

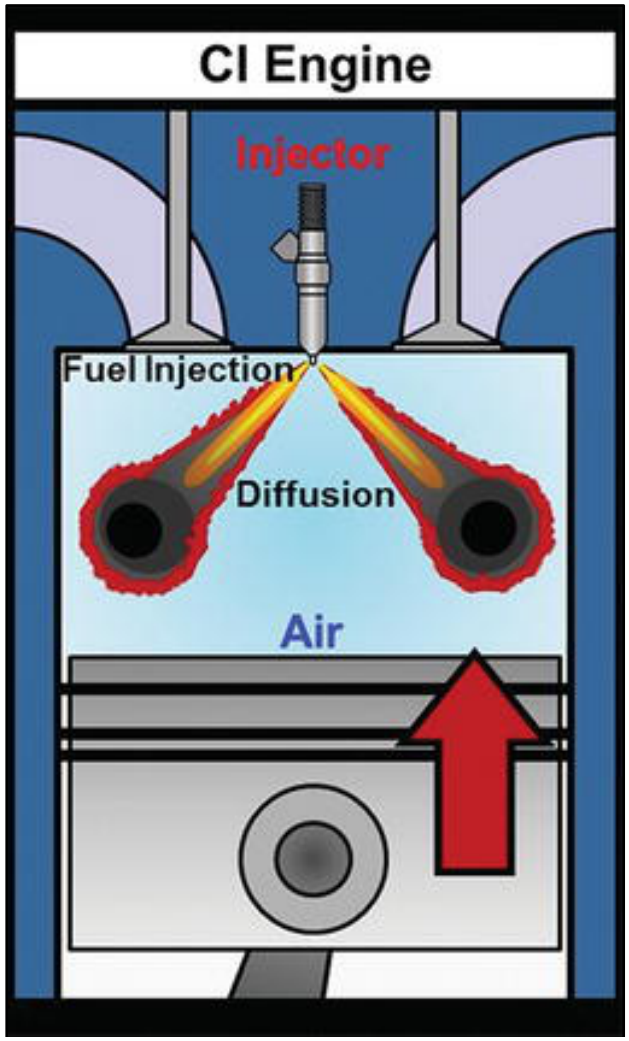


Figure 4.3: Diagram of stratified charge compression ignition (SCCI) [12]

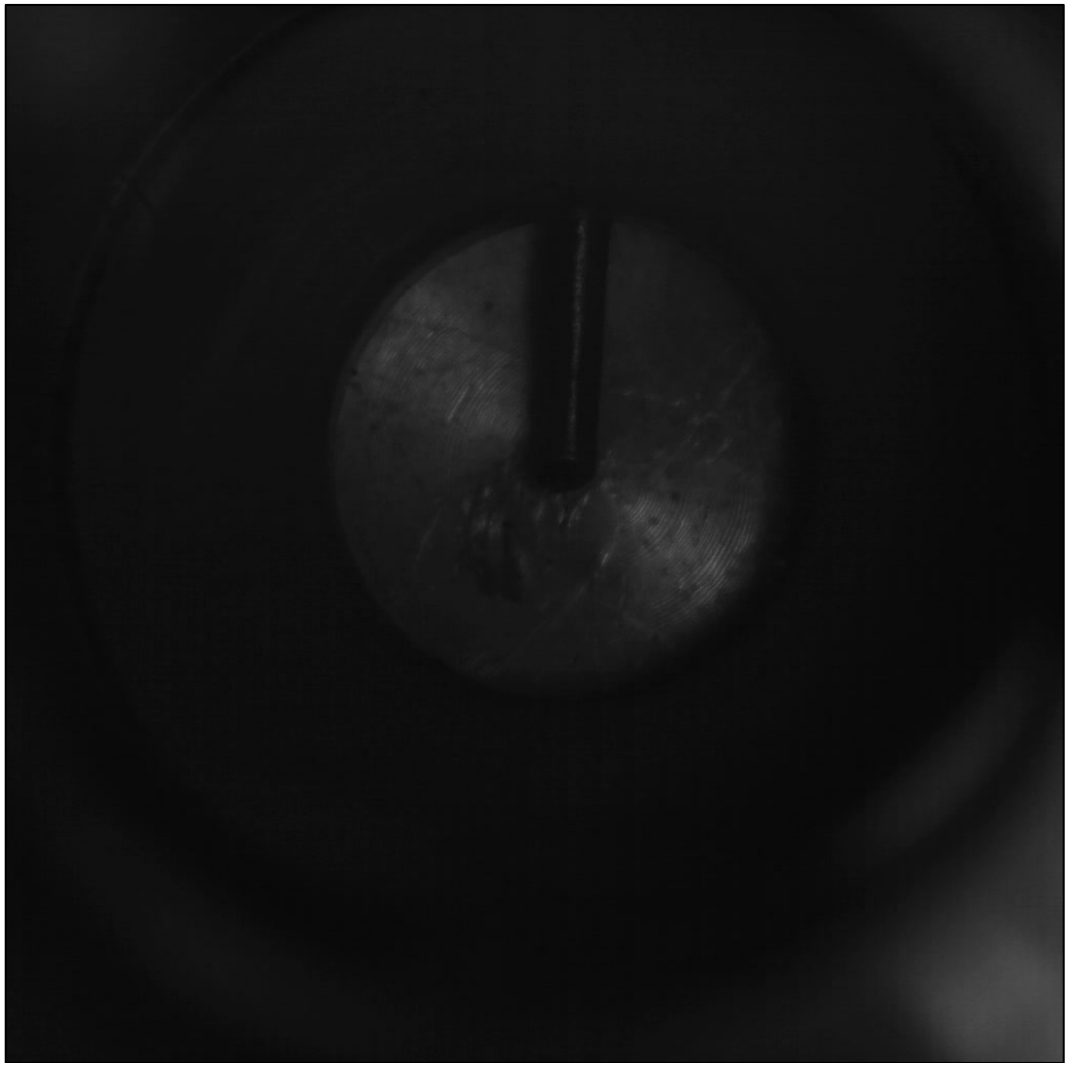

Figure 4.4: Frame from high-speed video just before the ignition of rich HCCI

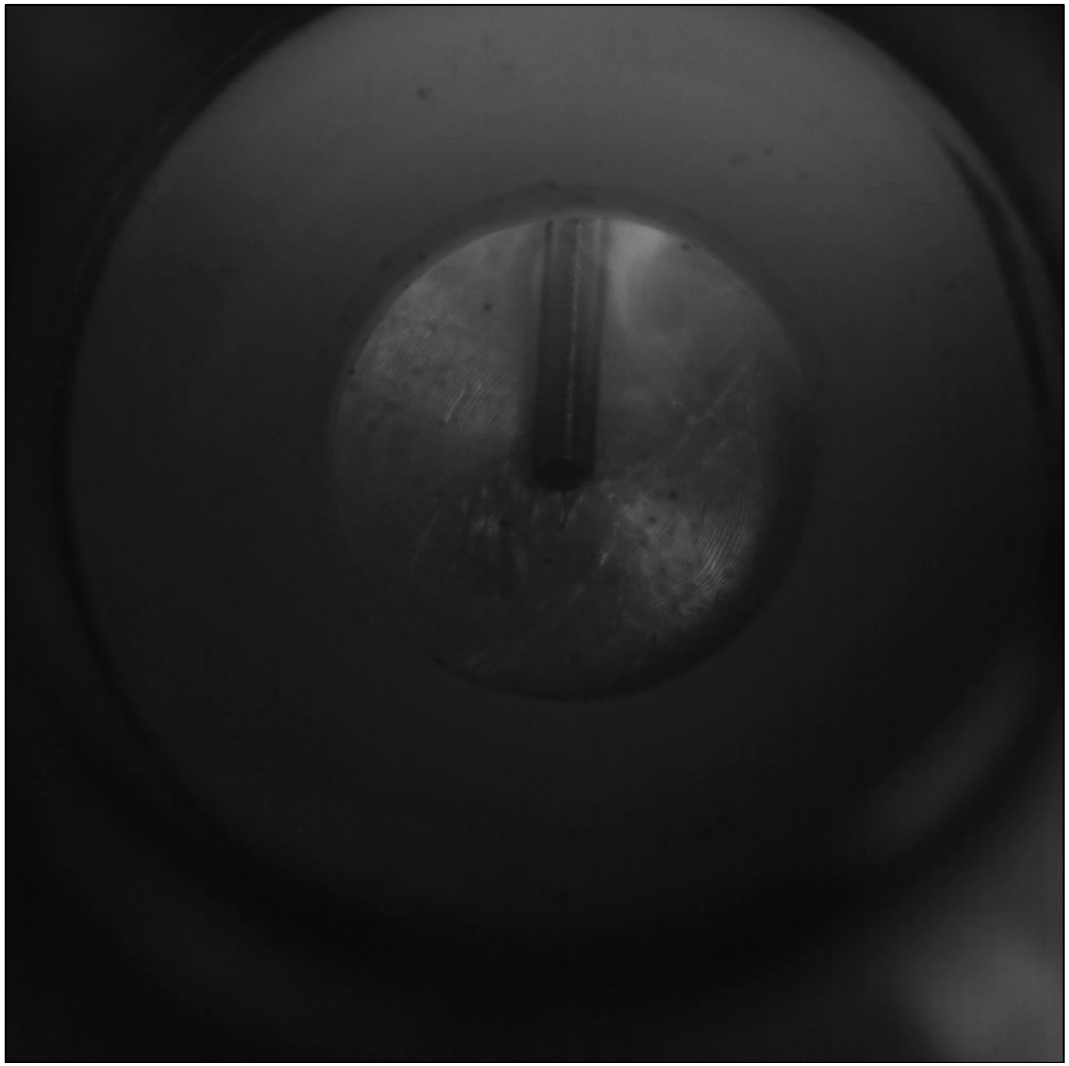

Figure 4.5: Frame from high-speed video of the ignition of rich HCCI

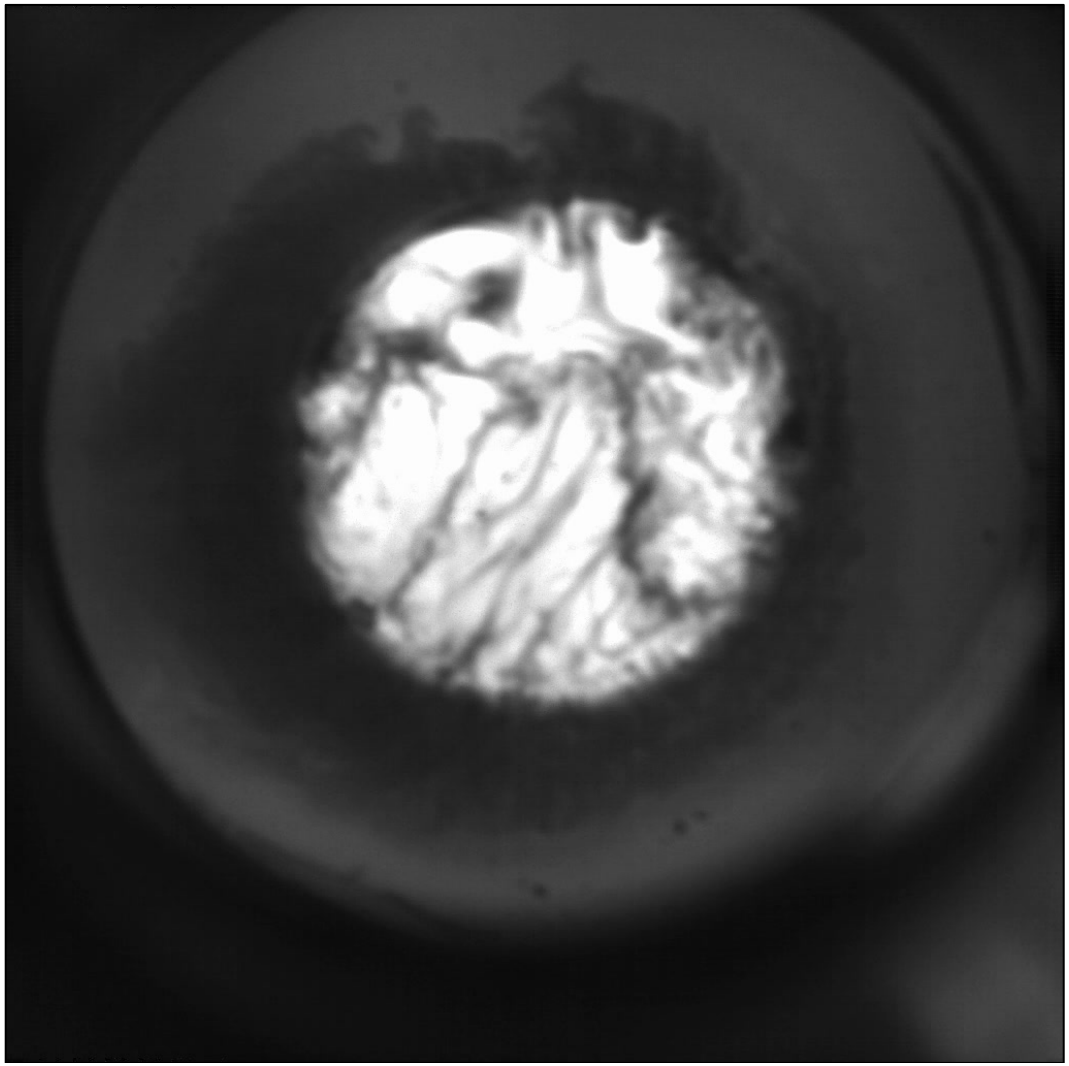

Figure 4.6: Frame from high-speed video just after the ignition of rich HCCI

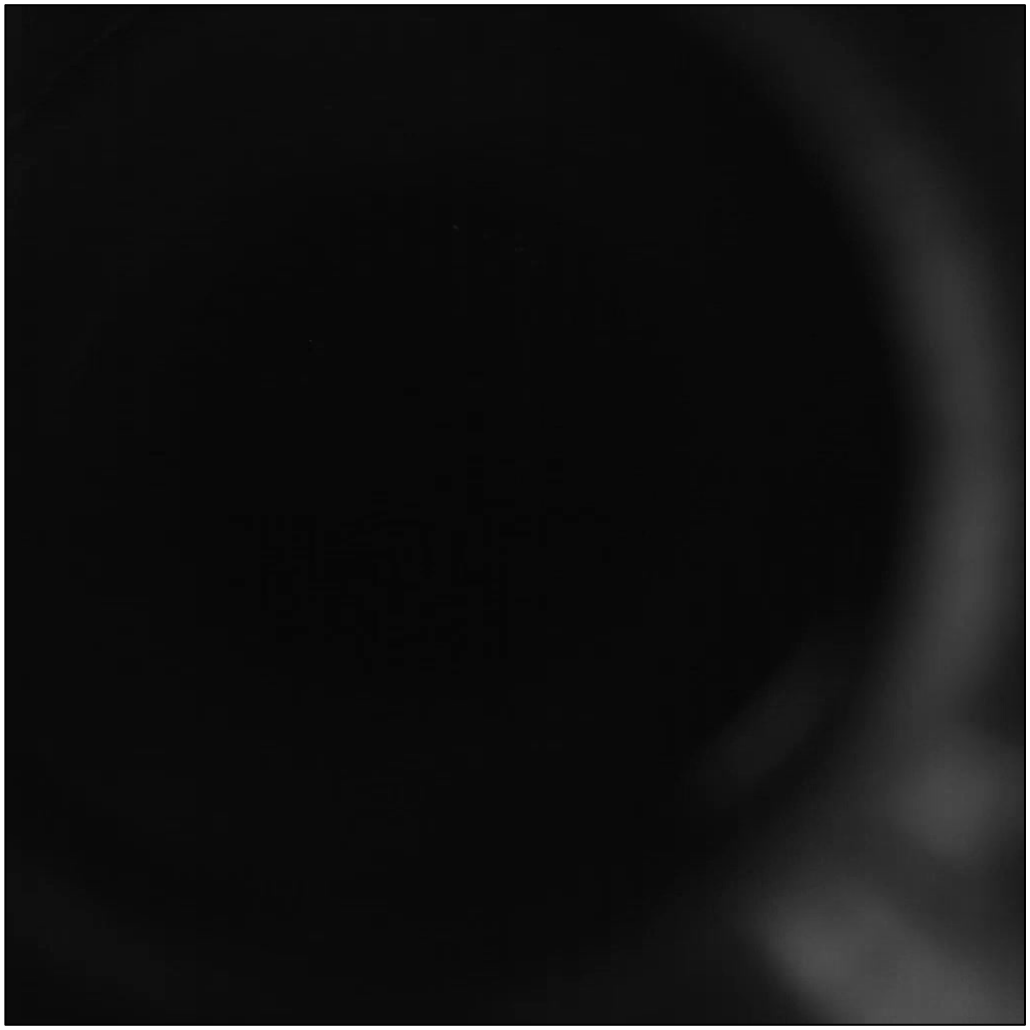

Figure 4.7: Frame from high-speed video just before the ignition of stoichiometric HCCI

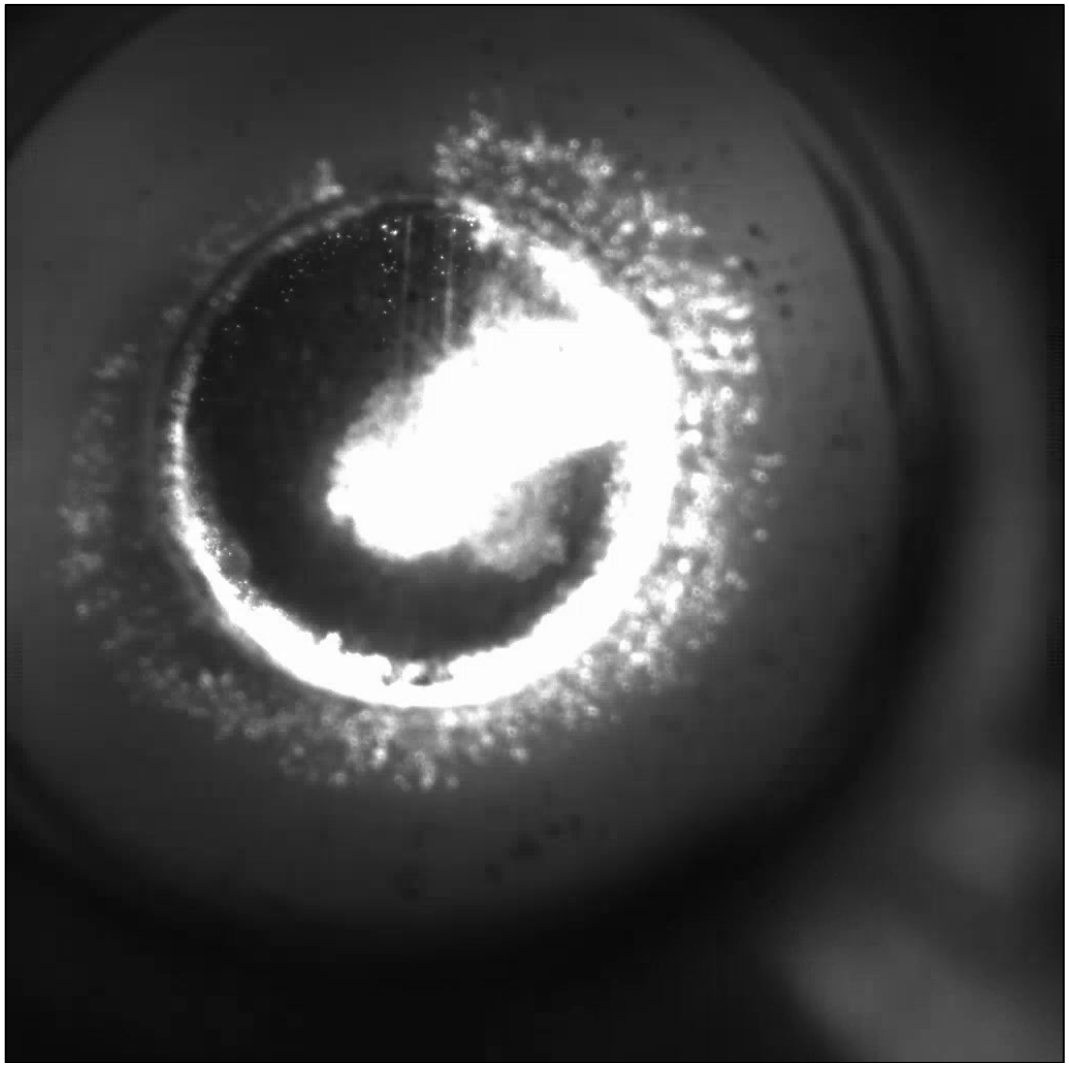

Figure 4.8: Frame from high-speed video of the ignition of stoichiometric HCCI

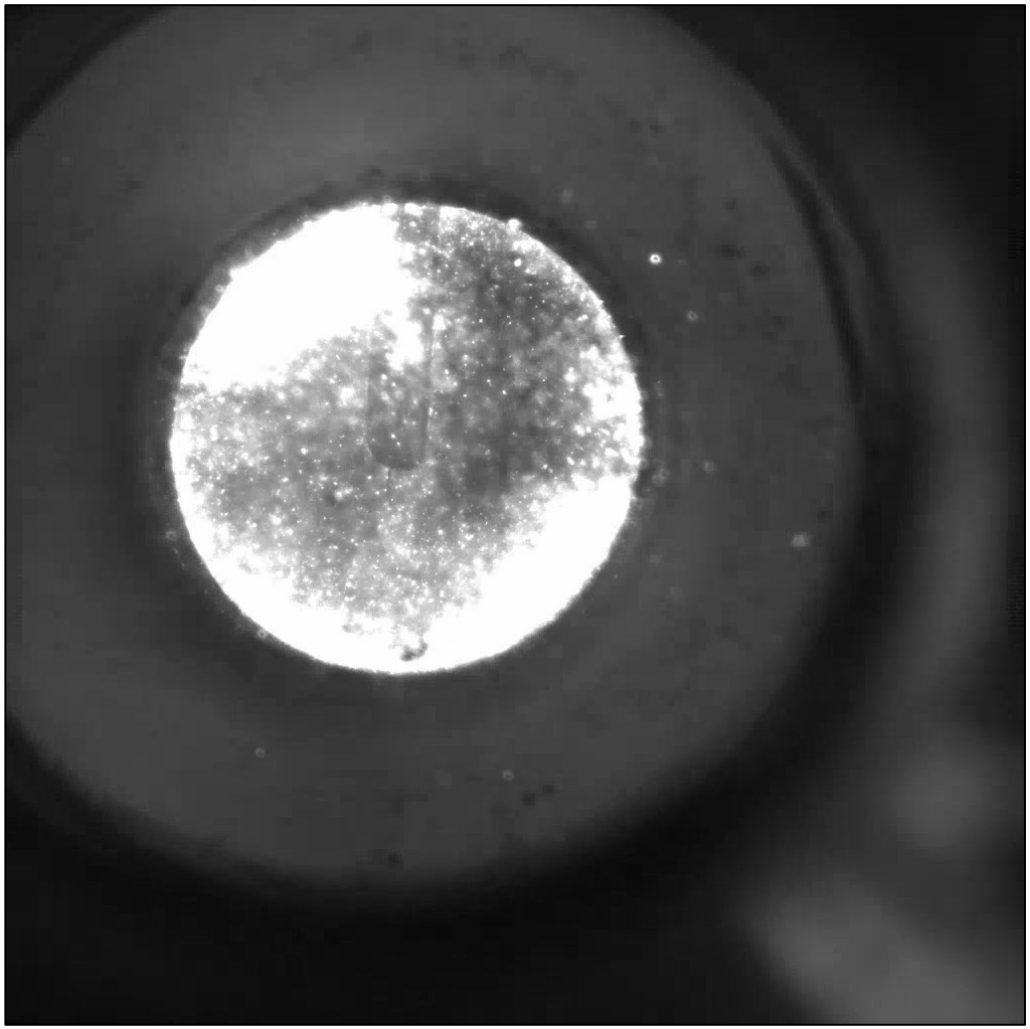

Figure 4.9: Frame from high-speed video just after the ignition of stoichiometric HCCI

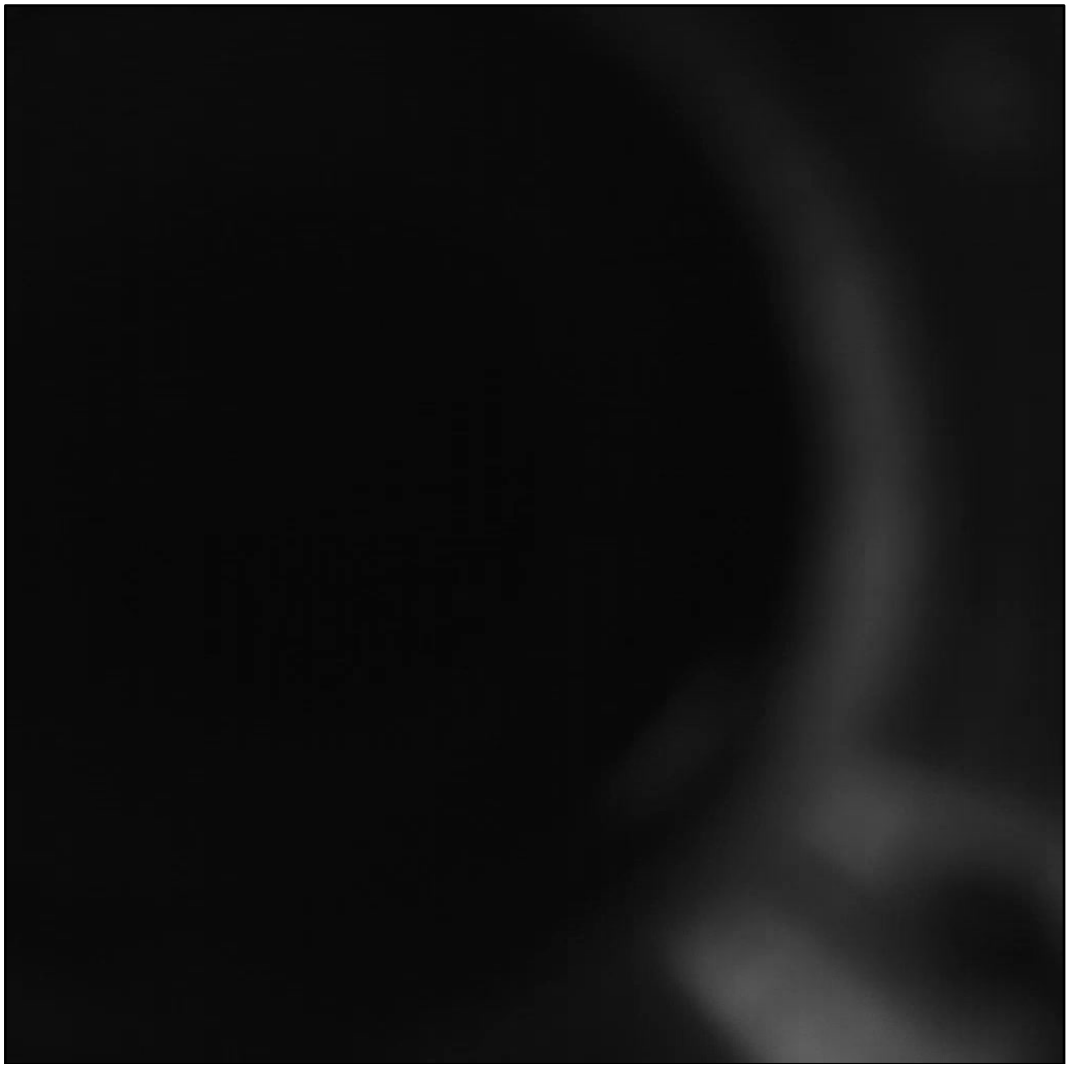

Figure 4.10: Frame from high-speed video just before the ignition of lean HCCI

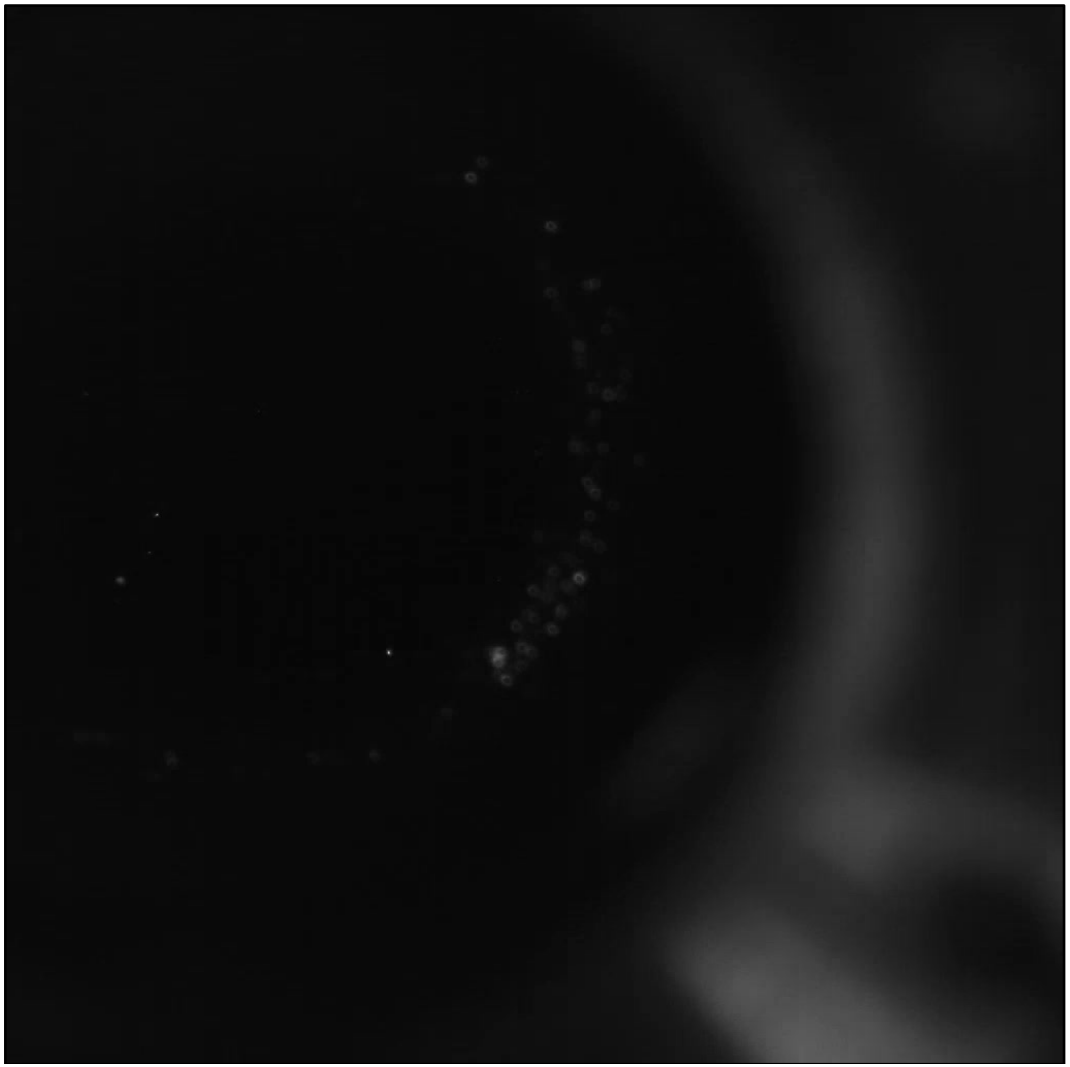

Figure 4.11: Frame from high-speed video of the ignition of lean HCCI

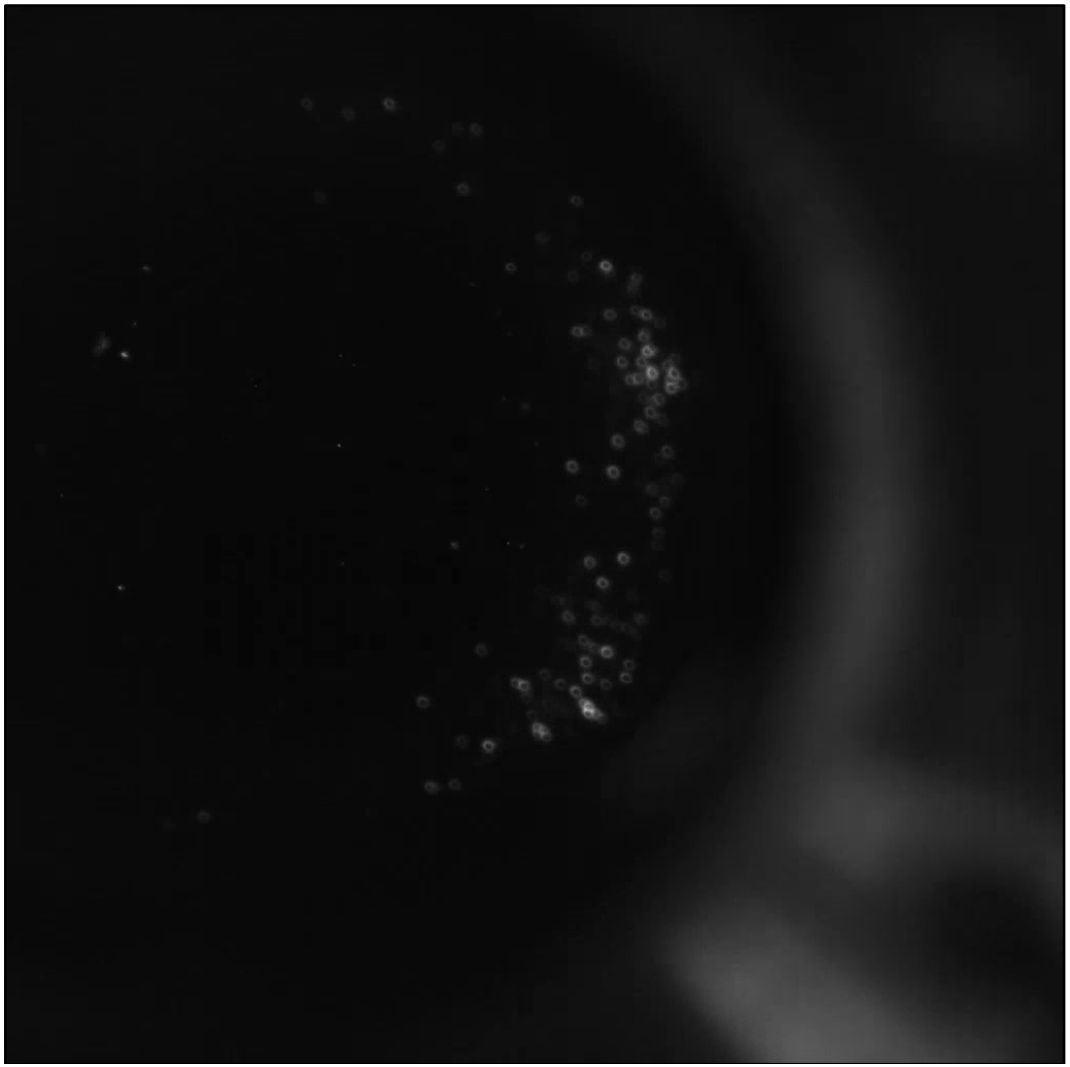

Figure 4.12: Frame from high-speed video just after the ignition of lean HCCI

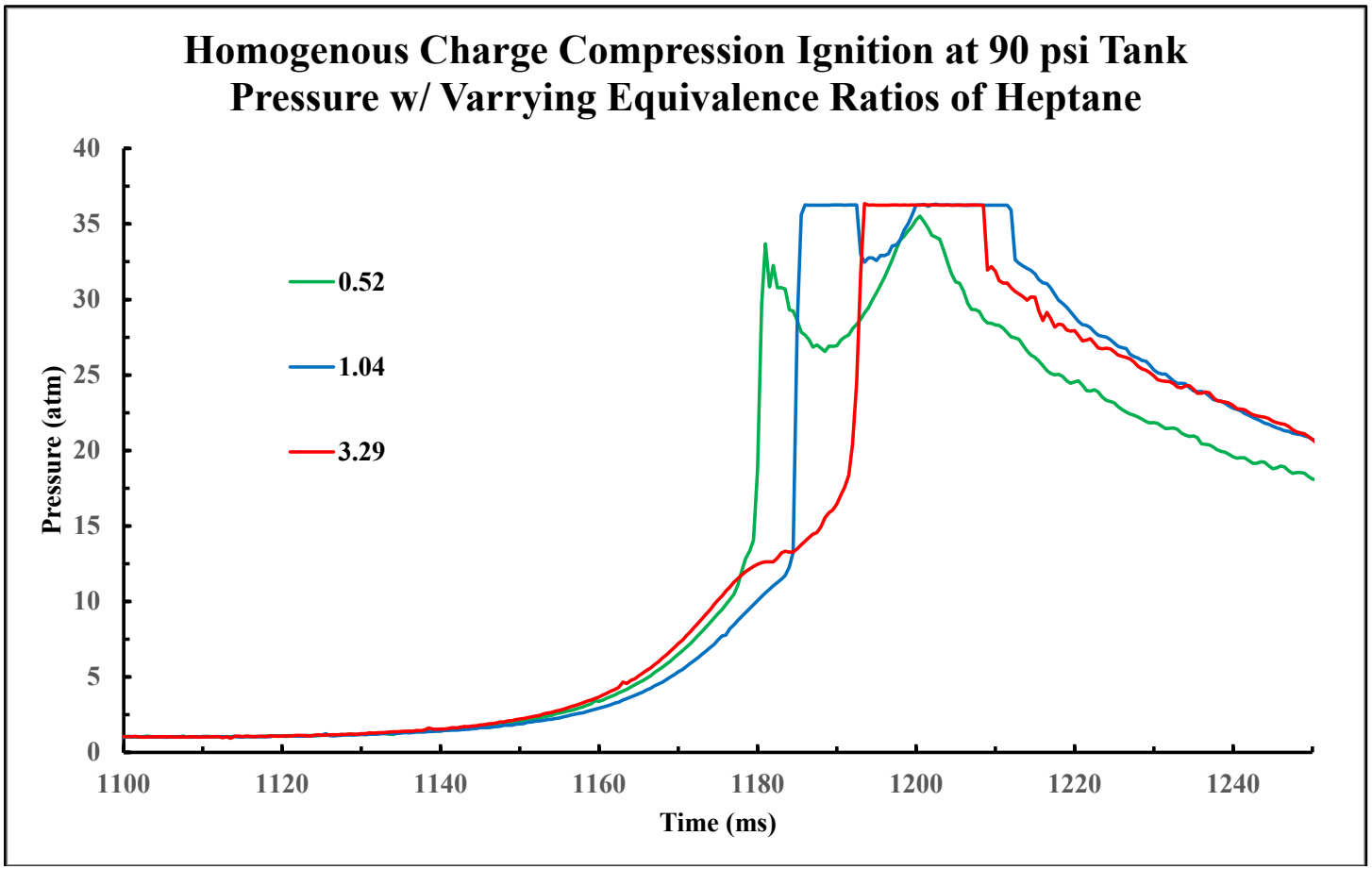


Figure 4.13: HCCI pressure curve comparison

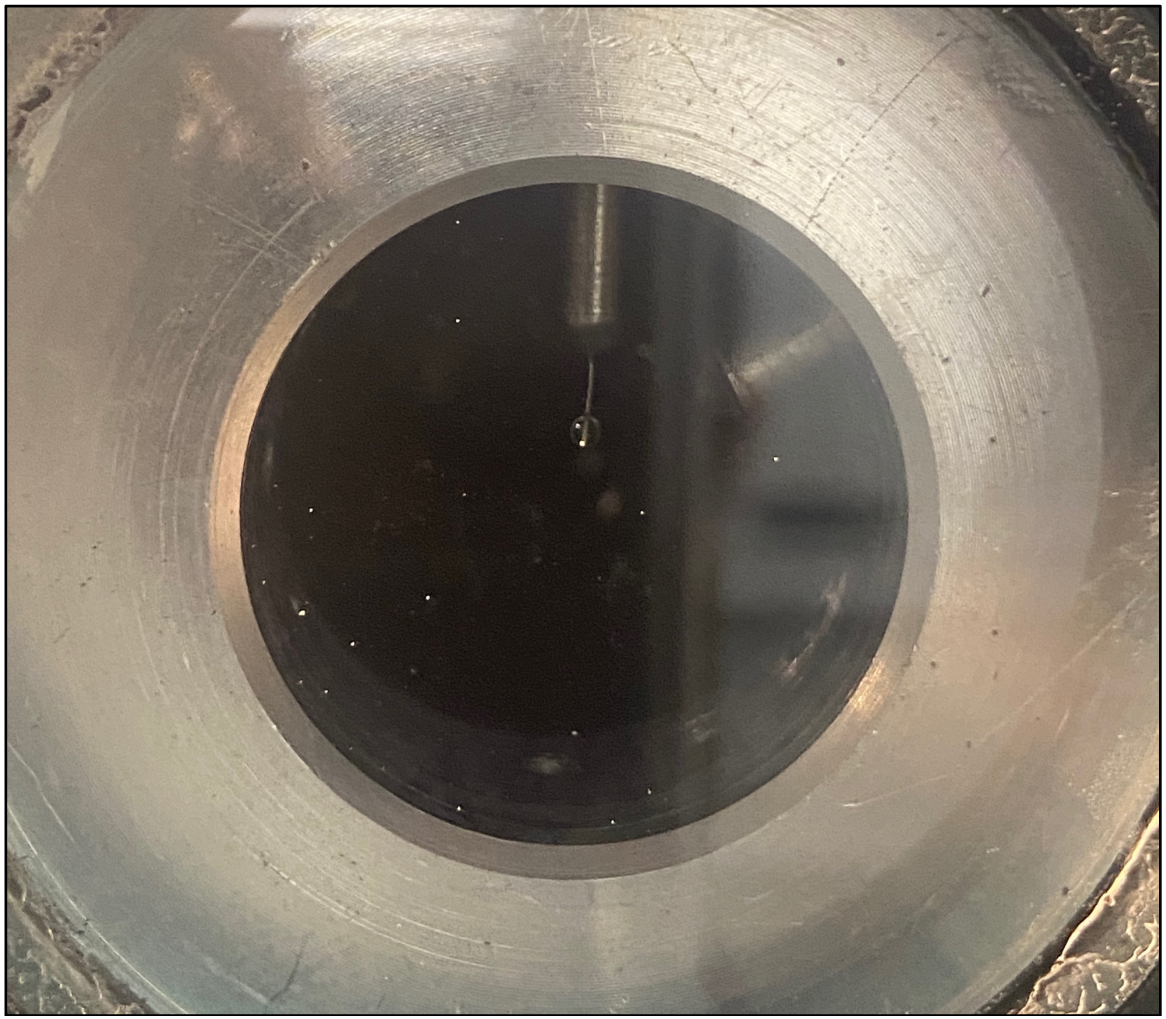

Figure 4.14: Tethered droplet suspended in center of window

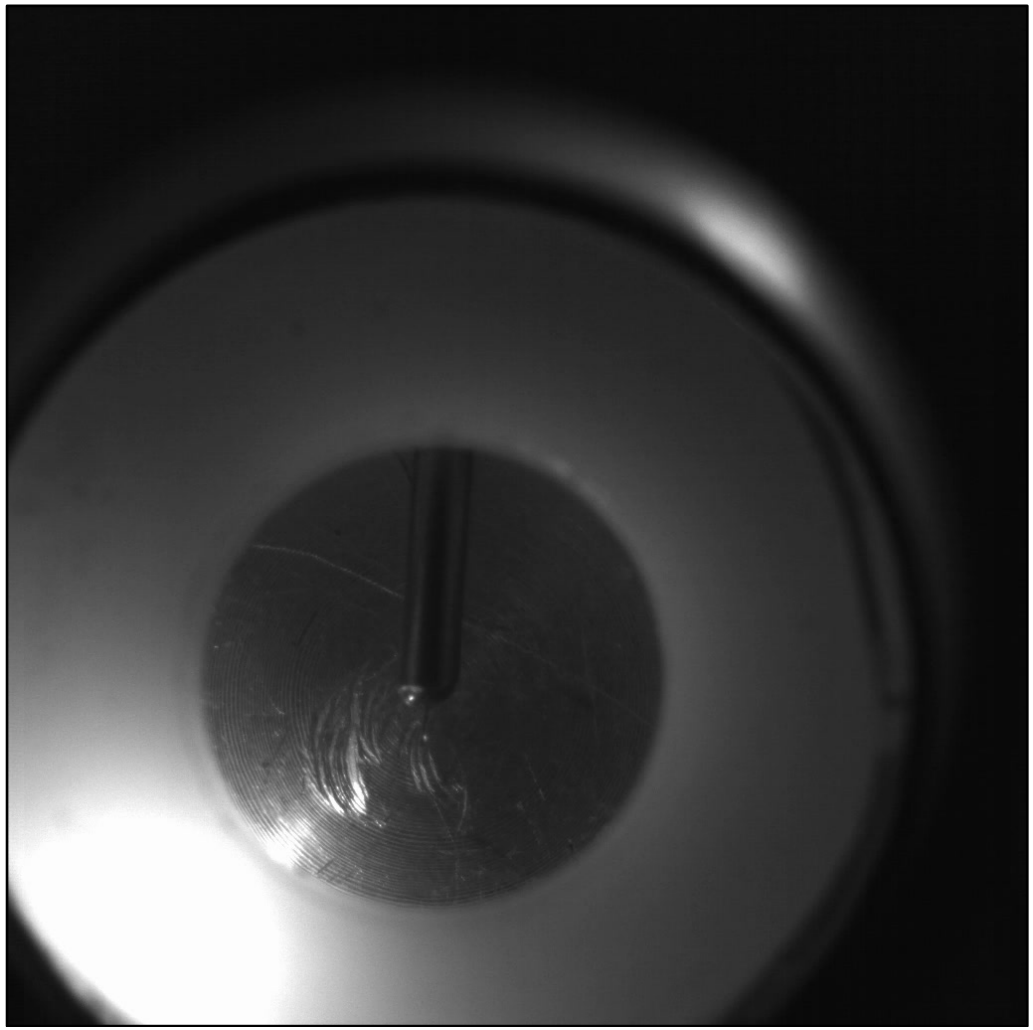

Figure 4.15: Frame from high-speed video of localized n-Heptane ignition during tethered droplet experiment

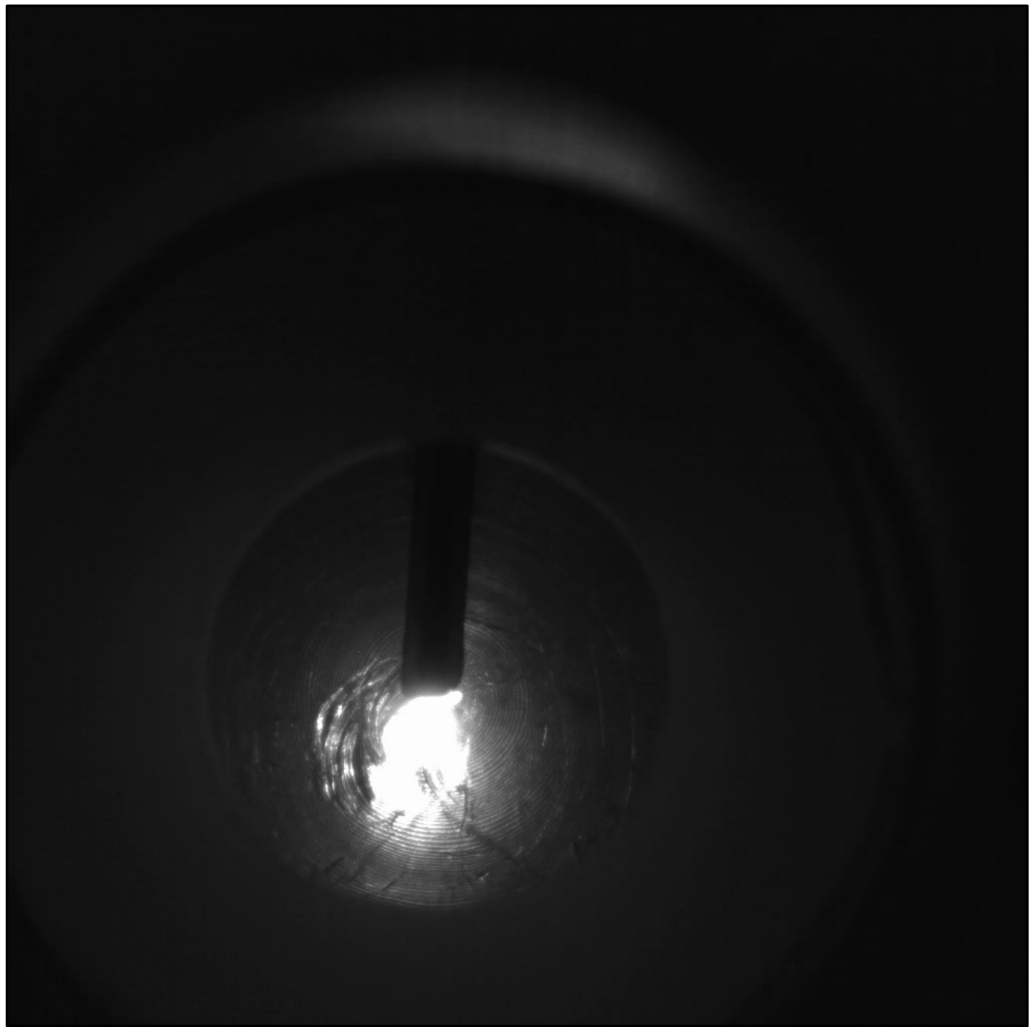

Figure 4.16: Frame from high-speed video of tethered n-Dodecane droplet ignition during tethered droplet experiment

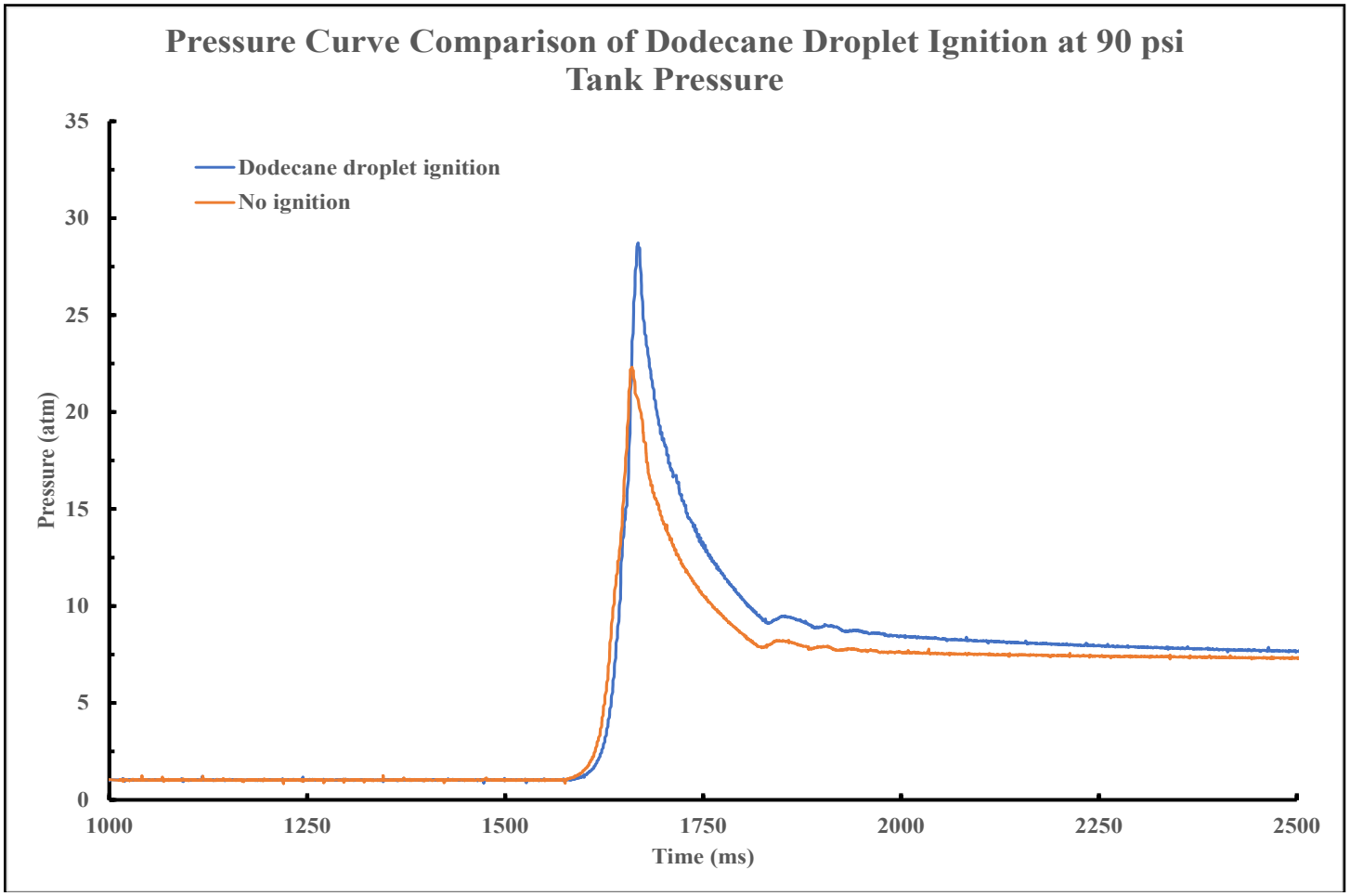


Figure 4.17: Pressure profile of tethered droplet ignition compared to non-reactive pressure profile

# CHAPTER 5

# CONCLUSION

The purpose of this RCEM was to develop a machine that can simulate the real-world conditions of a reciprocating, compression ignition engine. Even though this was not the first RCEM to be developed, very few have been created by other institutions. Traditionally, RCMs have been used to simulate the compression stroke of an engine, but they aren't without their limitations. RCMs, being linearly oriented, have difficulty in producing the correct acceleration profile as well as the difficulty in the inclusion of an expansion period. The RCEM fixes both of these issues by introducing a linear cam with a sinusoidal profile for compression and the ability to add an expansion period after the compression. After designing and assembling the RCEM, a number of issues arose in regard to leaking and stress caused by poor alignment. Multiple parts were redesigned to fix the alignment issues or to handle the amounts of stress. Several iterations of the RCEM's layout were done until it was verified to reliably produce repeatable compressions. Using the RCEM, two main experiments were performed, being HCCI and tethered droplet ignition, to collect some preliminary data that explores preferential vaporization and multiphase ignition.

The HCCI experiments that were run successfully showed that the ignition of fully vaporized, well-mixed n-Heptane could occur over a number of different equivalence ratios. This was important because n-Heptane is a common, low molecular weight hydrocarbon that is found in many fuels. Making sure n-Heptane could ignite in this device

was imperative to being able to explore more complex experiments. The tethered droplet ignition experiments successfully showed that liquid n-Dodecane droplets, experiencing a high enough temperature, can begin to vaporize and ignite. Due to the inability to further increase the compression ratio of the RCEM, the use of n-Heptane injected straight into the cylinder was required so that temperature could get high enough for n-Dodecane to vaporize. The pressure profile from the droplet ignition showed a much different curve when compared to the HCCI pressure curves. This experiment was important because it begins to show how the effects of multiphase ignition and preferential vaporization affect the overall combustion characteristics of a real fuel.

Although the information gathered from these experiments is fairly simple, it can be used to create new, more advanced experiments that further explore preferential vaporization and multiphase ignition. Some of these experiments include the categorization of the ignition of multi-component fuels and the introduction of $(NO)_x$ into the charge air within the cylinder to see how it affects combustion characteristics. The fundamental understanding of preferential vaporization and multiphase ignition has yet to be fully grasped, but these are necessary characteristics that will help with developing better fuels to be used in modern automotive engines and aerospace turbines.

# REFERENCES


[1] "Primary Energy Consumption by Source." *Our World in Data*, https://ourworldindata.org/grapher/primary-sub-energy-source?tab=chart&stackMode=absolute&time=2019®ion.

[2] "Statistical Review of World Energy: Energy Economics: Home." *Bp Global*, https://www.bp.com/en/global/corporate/energy-economics/statistical-review-of-world-energy.html.

[3] "OPEC Share of World Crude Oil Reserves." *OPEC*, https://www.opec.org/opec_web/en/data_graphs/330.htm.

[4] Stagni, A., et al. "The Role of Preferential Evaporation on the Ignition of Multicomponent Fuels in a Homogeneous Spray/Air Mixture." *Proceedings of the Combustion Institute*, vol. 36, no. 2, 2017, pp. 2483–2491., https://doi.org/10.1016/j.proci.2016.06.052.

[5] Mittal, Gaurav, and Chih-Jen Sung. "Aerodynamics inside a Rapid Compression Machine." *Combustion and Flame*, vol. 145, no. 1-2, Apr. 2006, pp. 160–180., https://doi.org/10.1016/j.combustflame.2005.10.019.

[6] Inc., Jack Kane; EPI. "- Piston Motion Basics -." *Piston Motion: The Obvious and Not-so-Obvious, by EPI, Inc.*, http://www.epi-eng.com/piston_engine_technology/piston_motion_basics.htm.

[7] Neuman, John, "Development of a Rapid Compression Controlled-Expansion Machine for Chemical Ignition Studies" (2015). Master's Theses (2009 -). Paper 290. http://epublications.marquette.edu/theses_open/290.

[8] "Ultra-Flat Extra Heavy Duty Table." *McMaster*, https://www.mcmaster.com/4769T585/.

[9] Mittal, Gaurav, and Chih-Jen Sung*. "A Rapid Compression Machine for Chemical Kinetics Studies at Elevated Pressures and Temperatures." *Combustion Science and Technology*, vol. 179, no. 3, 2007, pp. 497–530., https://doi.org/10.1080/00102200600671898.

[10] "Piezoelectric Pressure Sensor (PE - 250 Bar / 3625 Psi)." *Measurement Systems and Sensors*, https://www.kistler.com/en/product/type-601caa/.

[11] "Pressure: Pressure Sensor: G2 Pressure Transducer." *Ashcroft*, 5 Apr. 2021, https://www.ashcroft.com/products/pressure/pressure-sensors/g2-pressure-transducer/.

[12] Jung, Dongwon. "Autoignition and Chemical-Kinetic Mechanisms of Homogeneous Charge Compression Ignition Combustion for the Fuels with Various Autoignition Reactivity." *Advanced Chemical Kinetics*, 2018, https://doi.org/10.5772/intechopen.70541.

[13] *Heptane*, National Institute of Standards and Technology, https://webbook.nist.gov/cgi/cbook.cgi?ID=C142825&Mask=4#Thermo-Phase.

[14] *Dodecane*, National Institute of Standards and Technology, https://webbook.nist.gov/cgi/cbook.cgi?ID=C112403&Mask=4#Thermo-Phase.